

# A Polyaromatic Terdentate Binding Unit with Fused 5,6-Membered Chelates for Complexing s-, p-, d-, and f-Block Cations

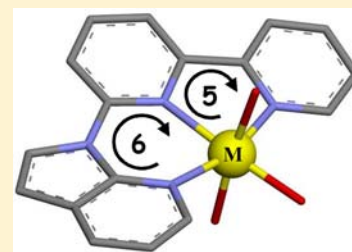
Thi Nhu Y Hoang,<sup>\*,†</sup> Marie Humbert-Droz,<sup>†</sup> Thibault Dutronc,<sup>†</sup> Laure Guénée,<sup>‡</sup> Céline Besnard,<sup>‡</sup> and Claude Piguet<sup>\*,†</sup>

<sup>†</sup>Department of Inorganic, Analytical and Applied Chemistry, University of Geneva, 30 quai E. Ansermet, CH-1211 Geneva 4, Switzerland

<sup>‡</sup>Laboratory of Crystallography, University of Geneva, 24 quai E. Ansermet, CH-1211 Geneva 4, Switzerland

## S Supporting Information

**ABSTRACT:** The polyaromatic terdentate ligand 6-(azaindol-1-yl)-2,2'-bipyridine (L7) combines one 5-membered chelate ring with a fused 6-membered chelate ring. It is designed to provide complexation properties intermediate between 2,2';6',2''-terpyridine (L1) (two fused 5-membered chelate rings) and 2,6-bis(azaindol-1-yl)pyridine (L6) (two fused 6-membered chelate rings). In polar organic solvents, L7 displays remarkable affinities for the successive fixation of two small univalent cations  $M = H^+$  or  $Li^+$ , leading to stable  $[M_m(L7)]^{m+}$  ( $m = 1-2$ ) complexes. Upon reaction with  $M = Mg^{2+}$  or  $Zn^{2+}$  cations, the large positive charge densities borne by the metals result in the successive cooperative complexation of two ligands to give  $[M(L7)_n]^{n+}$  ( $n = 1-2$ ). For small  $Sc^{3+}$ , unavoidable traces of water favor the formation of the protonated ligand at millimolar concentrations in acetonitrile, but the use of larger  $Y^{3+}$  cations leads to  $[Y(L7)_n]^{n+}$  ( $n = 1, 2$ ), for which stability constants of  $\log(\beta_{1,1}^{Y,L7}) = 2.9(5)$  and  $\log(\beta_{1,2}^{Y,L7}) = 5.3(4)$  are estimated. The complexation behaviors are supported by speciations in solution, thermodynamic analyses, and solution and solid-state structures.



## INTRODUCTION

Molecular mechanics have established that aliphatic 5-membered chelate rings were geometrically adapted for catching large cations, whereas six-membered analogues matched smaller metals (see Figure S1 in the Supporting Information).<sup>1</sup> In order to improve structural control and light-harvesting properties, aromatic rings were incorporated into the chelating ligands and numerous large trivalent lanthanide cations, Ln(III), acting as luminescent<sup>2</sup> or magnetic<sup>3</sup> probes, were successfully coordinated not only with 5-, but also with 6- or even with 7-membered polyaromatic chelates, in contradiction with the original rule of thumb.<sup>2</sup> However, we note that 6- and 7-membered chelates, which are geometrically poorly adapted for large Ln(III), systematically relied on negatively charged ligands in order to benefit from the considerable entropic driving force produced by the charge neutralization accompanying the complexation process in polar solvents.<sup>1b,4</sup> For neutral polyaromatic terdentate ligands, only fused 5-membered chelates are known to give stable complexes with trivalent Ln(III), among which the terdentate ligands L1,<sup>5</sup> L2,<sup>6</sup> L3,<sup>7</sup> L4,<sup>8</sup> and L5<sup>9</sup> are the archetypes (see Scheme 1).

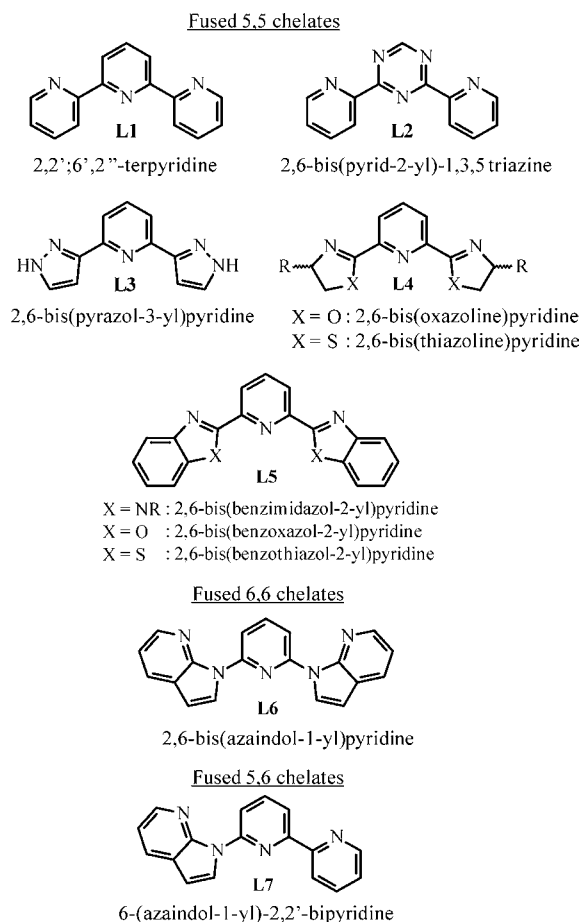
Beyond the investigation of these neutral soft receptors for the selective extraction of actinides over lanthanides in acidic nuclear wastes, only slight interest was focused on their potential selectivity along the lanthanide series. For terpyridine L1, the fixation of the first binding unit gives moderately stable  $[Ln(L1)(H_2O)_n]^{3+}$  complexes in water, whose formation constants stepwise increase along the series ( $\log(\beta_{1,1}^{Ln,L1}) = 2.08-2.80$  for Ln = La, Eu, Lu).<sup>5f</sup> In less-polar acetonitrile, the

stability is improved by 5 orders of magnitude ( $\log(\beta_{1,1}^{Ln,L1}) = 7.5-7.7$ ), but the size-discriminating effects are leveled out.<sup>5h</sup> To the best of our knowledge, only the third successive thermodynamic constants  $K_{1,3}^{Ln,L5}$ , transforming  $[Ln(L5)_2(CH_3CN)_3]^{3+}$  into  $[Ln(L5)_3]^{3+}$ , display some noticeable size selectivity along the lanthanide series. These constants decrease by 3 orders of magnitude in going from Ln = Gd(III) to Lu(III), because of the steric constraints produced by the helical wrapping of the three strands in the final complexes.<sup>5t,9d</sup> With this in mind, we suspect that the large distortion of the polyaromatic backbone detected upon meridional ter-coordination of L6 (fused 6,6-membered chelate) to Zn(II)<sup>10</sup> or Cu(II),<sup>11</sup> compared with the coplanar arrangement found for L1 (fused 5,5-membered chelate) in  $[Zn(L1)Br_2]$ ,<sup>12</sup> could produce unusual thermodynamic effects. Along this line of reasoning, we note that L6 indeed reacts with  $YI_3$  under anhydrous conditions to give  $[Y(L6)_n]^{3+}$  ( $n = 1, 2$ ), despite its claimed reluctance for large cations; however, the extreme sensitivity of these complexes to moisture and their low solubility prevent further investigations.<sup>10</sup> Pushing forward this strategy, we report here on the preparation of the unsymmetrical terdentate aromatic ligands L7, which are made of a 5-membered bipyridine chelate fused with a 6-membered pyridine-azaindole ring,<sup>13</sup> and we also explore its complexation properties with spherical cations possessing various  $Z^2/R$

Received: March 1, 2013

Published: April 19, 2013

**Scheme 1. Chemical Structures of the Terdentate Polyaromatic Ligands L1–L7 in Their Relaxed *trans*–*trans* Conformations**



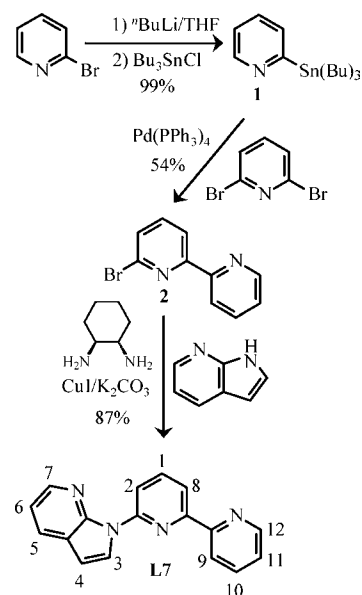
electrostatic factors ( $Z$  is the charge of the cation in electrostatic units and  $R$  is its ionic radius).

## RESULTS AND DISCUSSION

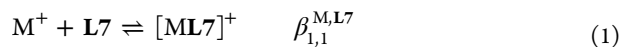
**Synthesis of Ligand L7, and Complexation with Univalent  $H^+$  and  $Li^+$  Cations.** The terdentate ligand L7 is obtained in two steps from 2-(tributylstannyl) pyridine (**1**) with a 47% global yield (see Scheme 2). The initial Stille coupling reaction uses commercially available 2,6-dibromopyridine to give 6-bromo-2,2'-bipyridine (**2**),<sup>14</sup> which is transformed to L7 via a catalyzed Ullmann-type coupling reaction with 7-azaindole.<sup>15</sup> The 12 aromatic  $^1H$  NMR signals of L7 (see Figure 2 and Figures S2–S5 in the Supporting Information) are compatible with an average planar  $C_s$  symmetry, where the distal N atoms adopt *trans*–*trans* conformations, with respect to the nitrogen of the central pyridine ring, as shown in Scheme 2. The low-field resonances of H2–H3 and H8–H9 pairs are diagnostic for their location close to the electronegative N atoms of the adjacent heterocyclic ring (see Tables S1 and S2 in the Supporting Information), while the lack of a nuclear Overhauser enhancement effect between the H atoms of each hydrogen pair precludes *cis*–*cis* geometry.

$^1H$  NMR titrations of L7 in  $CD_3CN/CDCl_3$  (1:1) or in  $CD_3CN$  with  $CF_3SO_3H$  (Figures S2 and S3 in the Supporting Information) or with  $LiClO_4$  (Figures S4 and S5 in the Supporting Information) exhibit fast-exchange processes on the

**Scheme 2. Synthesis of Ligand L7 with Numbering Scheme for NMR Data**



NMR time scale with end points for  $M:L7 = 1.0$  and  $2.0$ , in agreement with the formation of the  $[ML7]^+$  and  $[M_2(L7)]^{2+}$  complexes detected by ESI-MS in the gas phase (see Table S3 in the Supporting Information). The complete set of dynamically average chemical shifts can be satisfyingly fitted to eqs 1 and 2, using nonlinear least-squares techniques, to give  $\log(\beta_{1,1}^{M,L7})$  and  $\log(\beta_{2,1}^{M,L7})$  (Table 1),<sup>16</sup> ligand distributions (Figure 1 and Figure S6 in the Supporting Information) and individual  $^1H$  NMR spectra (see Figure 2, as well as Figure S7, Table S1, and Table S2 in the Supporting Information).



As expected, the formation constants  $\beta_{m,1}^{M,L7}$  are reduced by a factor of 5–10 in pure  $CD_3CN$ , because of the larger solvation of the free cations in a more polar solvent. Compared with L1 ( $\log(\beta_{1,1}^{H,L1}) = 3.4(1)$  and  $\log(\beta_{2,1}^{H,L1}) = 5.3(3)$ ) and with L6 ( $\log(\beta_{1,1}^{H,L6}) = 5.3(3)$  and  $\log(\beta_{2,1}^{H,L6}) = 8.9(3)$ ) in  $CD_3CN/CDCl_3$  (1:1),<sup>10</sup> L7 displays the largest affinity for protons ( $\log(\beta_{1,1}^{H,L7}) = 5.7(1)$  and  $\log(\beta_{2,1}^{H,L7}) = 9.5(5)$ ), together with non-negligible formation constants with  $Li^+$ , for which L1 and L6 exhibited nonmeasurable stability constants at millimolar concentrations. The careful analysis of the individual  $^1H$  NMR spectra gives pertinent structural information. Upon titration with  $H^+$ , the concomitant downfield shift of the signals of H2, H3, and H5 indicates a decrease in electronic density upon protonation, but the *trans* conformation of the azaindol-pyridine unit is not seriously affected by the fixation of the first proton in  $[HL7]^+$  (red arrows in Figure 2).

In contrast, the upfield shift of H8 (–0.15 ppm) points to a *cis* conformation of the 2,2'-bipyridine unit in  $[HL7]^+$ , because H8 is no more influenced by the N atom of the adjacent pyridine ring,<sup>10</sup> while the concomitant downfield shift of H10 (0.73 ppm) demonstrates that protonation occurs on the distal pyridine ring (blue arrows in Figure 2).<sup>17</sup> The second protonation occurs at the azaindol ring and leads to a twisted *cis*–*cis* conformation for the terdentate ligand in  $[H_2L7]^{2+}$ . With  $M = Li^+$ , the concomitant downfield shift of the signals of

**Table 1. Cumulative Thermodynamic Constants ( $\log(\beta_{ML7}^{ML7})$ , Associated Microscopic Affinities ( $\log(\beta_{ML7}^{ML7})$ ), Intramolecular Intermetallic ( $\log(\beta_{ML7}^{ML7})$ ) and  $\Delta G_{\text{interaction}}^{ML7}$ ) and Interligand ( $\log(\beta_{ML7}^{ML7})$ ) and  $\Delta G_{\text{interaction}}^{ML7}$ ) Interactions and Allosteric Cooperativity Factors ( $\alpha$ ) Obtained by  $^1\text{H}$  NMR for the Titrations of L7 with  $\text{CF}_3\text{SO}_3\text{H}$ ,  $\text{LiClO}_4$ ,  $\text{Mg}(\text{ClO}_4)_2$ ,  $\text{Zn}(\text{CF}_3\text{SO}_3)_2$ , and  $\text{Y}(\text{CF}_3\text{SO}_3)_3 \cdot \text{diglyme}$  at 298 K**

	$\text{H}^+$		$\text{Li}^+$		$\text{Mg}^{2+}$		$\text{Zn}^{2+}$		$\text{Y}^{3+}$
	$\text{CD}_3\text{CN}/\text{CDCl}_3$ (1:1)	$\text{CD}_3\text{CN}$	$\text{CD}_3\text{CN}/\text{CDCl}_3$ (1:1)	$\text{CD}_3\text{CN}$	$\text{CD}_3\text{CN}/\text{CDCl}_3$ (1:1)	$\text{CD}_3\text{CN}$	$\text{CD}_3\text{CN}/\text{CDCl}_3$ (1:1)	$\text{CD}_3\text{CN}$	
$\log(\beta_{1,1}^{ML7})$	5.7(1)	5.3(2)	3.4(1)	2.6(1)	4.1(3)	3.1(4)	4.0(2)	3.8(2)	2.9(5)
$\log(\beta_{2,1}^{ML7})$	9.5(5)	9.1(2)	6.5(2)	5.5(2)	8.8(2)	7.6(5)	6.2(2)	6.3(1)	5.3(4)
$\log(\beta_{\text{connect}}^{ML7})$	5.4(1)	4.8(2)	2.3(2)	1.5(1)	2.7(3)	1.8(4)	2.6(2)	2.4(2)	2.1(4)
$\Delta G_{\text{connect}}^{ML7}$ ( $\text{kJ mol}^{-1}$ )	-30.8(6)	-28.5(1.1)	-13.2(1.1)	-8.7(6)	-15.4(1.9)	-10.0(2.0)	-15.0(1.1)	-13.8(1.1)	-12.1(2.9)
$\log(\beta_{1,1}^{ML7})$	-1.4(5)	-1.2(4)	-0.3(4)	0.3(2)	2.0(2.0)	3.0(8)	-0.4(4)	0.1(3)	0.3(8)
$\Delta E_{\text{interaction}}^{ML7}$ ( $\text{kJ mol}^{-1}$ )	9.1(3.0)	6.8(2.0)	1.7(2.0)	-1.7(1.4)	-11.7(11.4)	-17.3(4.3)	2.4(2.0)	-0.5(1.7)	-1.6(4.6)
$\alpha^a$	0.03(5)	0.06(5)	0.5(4)	2.0(1.1)	100(460)	1000(1840)	0.4(4)	1.3(9)	2.0(3.7)

<sup>a</sup>Equation taken from ref 21.  $\alpha = [(\omega_{1,1}^{ML7})^2 / (\omega_{2,1}^{ML7})^2] \times [\beta_{2,1}^{ML7} / (\beta_{1,1}^{ML7})^2] = \beta_{1,2}^{ML7} / (\beta_{1,1}^{ML7})^2$ . <sup>b</sup>Equation taken from ref 21.  $\alpha = [(\omega_{1,1}^{ML7})^2 / (\omega_{1,2}^{ML7})^2] \times [\beta_{1,2}^{ML7} / (\beta_{1,1}^{ML7})^2] = \beta_{1,2}^{ML7}$ .

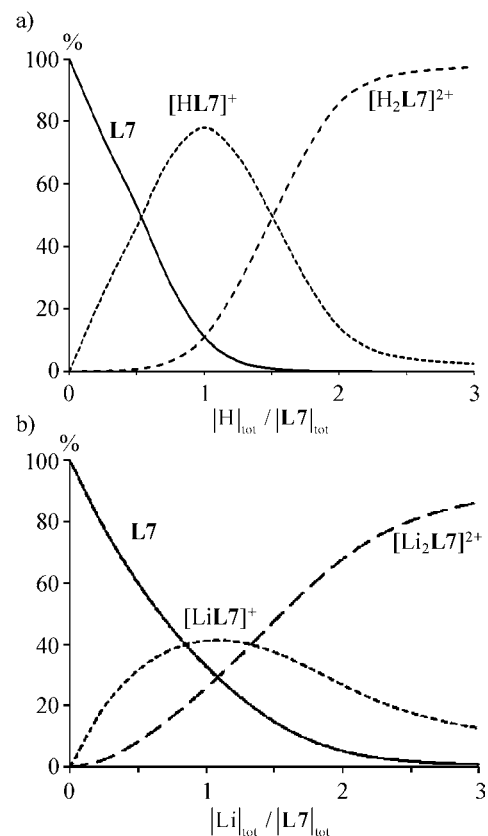


**Figure 1.** Computed ligand speciation (mole fraction (%)) of the ligand in the various species) for the titrations of L7 with (a)  $\text{CF}_3\text{SO}_3\text{H}$  and (b)  $\text{LiClO}_4$  in  $\text{CD}_3\text{CN}/\text{CDCl}_3$  (1:1) at 298 K. Total ligand concentration  $[\text{L7}]_{\text{tot}} = 7.5 \times 10^{-3}$  M.

H2–H3 and of H8–H9 in  $[\text{LiL7}]^{2+}$  implies a *cis-cis* conformation for the ligand upon fixation of the first  $\text{Li}^+$  cation. The affinity for a second  $\text{Li}^+$  cation remains modest and does not further significantly affect the  $^1\text{H}$  NMR spectrum (see Figure 2 and Figure S7 in the Supporting Information).

X-ray crystal structures solved for  $[\text{HL7}](\text{CF}_3\text{SO}_3)$  (**3**),  $[\text{H}_2\text{L7}](\text{ClO}_4)_2$  (**4**), and  $[\text{Li}(\text{L7})(\text{ClO}_4)(\text{H}_2\text{O})]$  (**5**) confirm the solution data with the coordinated polyaromatic terdentate unit adopting coplanar *trans-cis*  $[\text{HL7}]^+$ , twisted *cis-cis*  $[\text{H}_2\text{L7}]^{2+}$ , and coplanar *cis-cis*  $[\text{LiL7}]^+$  conformations (see Figure 3, as well as Figure S8 and Tables S4–S13 in the Supporting Information). The protonated cations  $[\text{HL7}]^+$  and  $[\text{H}_2\text{L7}]^{2+}$  are involved in weak intramolecular and intermolecular hydrogen bonds in the crystals of **3** and **4** (see Tables S7 and S10 in the Supporting Information). In **5**, the univalent Li metal displays standard Li–N distances<sup>18</sup> and its coordination sphere is completed with one water molecule and one unidentate perchlorate counteranion to give the five-coordinated pseudo-trigonal bipyramidal complex  $[\text{Li}(\text{L7})(\text{ClO}_4)(\text{H}_2\text{O})]$ .<sup>19</sup> Taking the molecular structures of *cis-cis*  $[\text{H}_2\text{L7}]^{2+}$  as a rough model for the meridional ter-coordination of this ligand around multivalent cations, we conclude that the shape of the irregular triangle drawn by the three donor N atoms (Figure 4) is intermediate between the pseudo-isosceles triangles reported for  $[\text{H}_2\text{L1}]^{2+}$  (adapted for large cations)<sup>20</sup> and  $[\text{H}_2\text{L6}]^{2+}$  (adapted for small cations).<sup>10</sup>

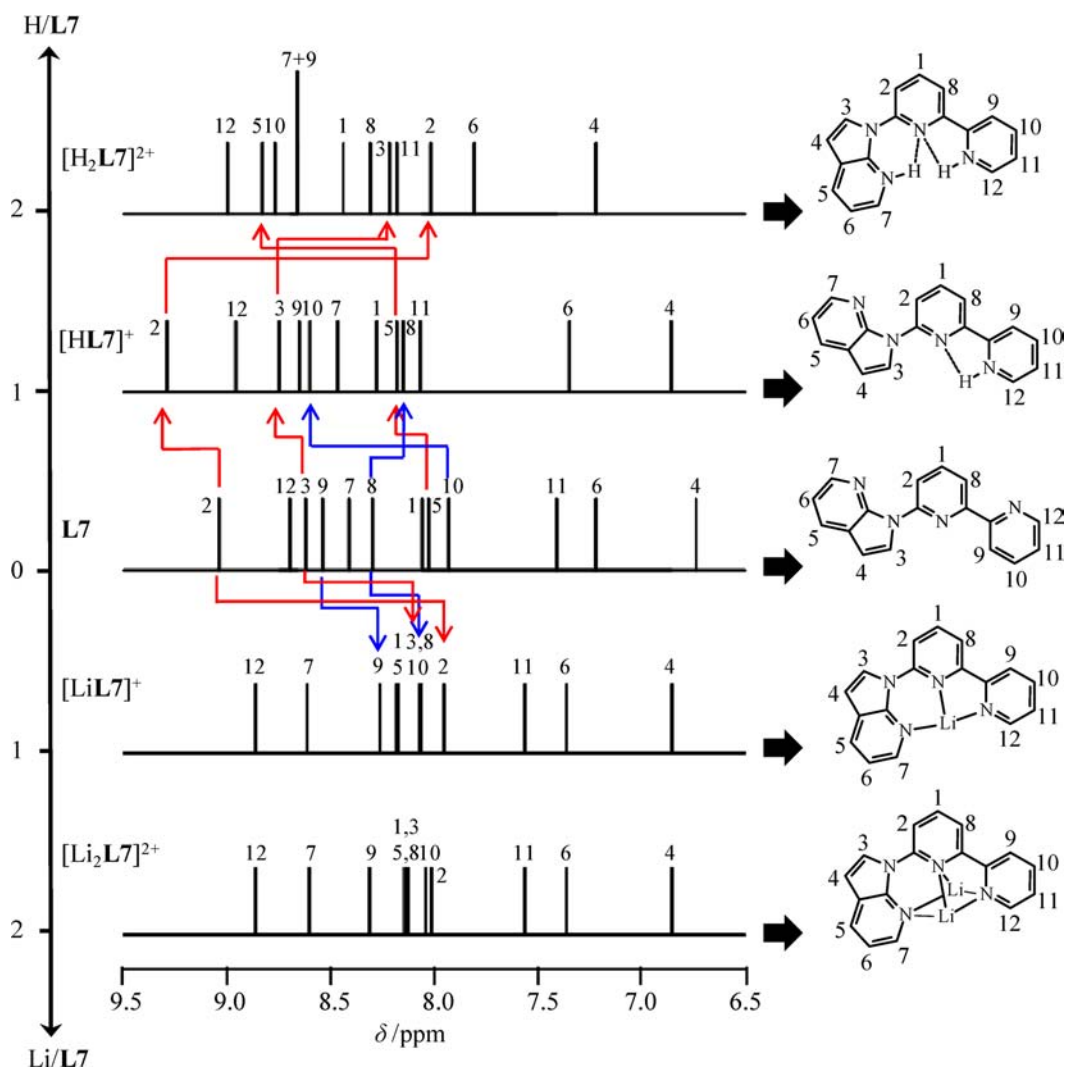


**Figure 2.** Computed individual  $^1\text{H}$  NMR spectra for  $\text{L7}$  (middle),  $[\text{HL7}]^+$  and  $[\text{H}_2\text{L7}]^{2+}$  (top), and  $[\text{LiL7}]^+$  and  $[\text{Li}_2\text{L7}]^{2+}$  (bottom) in  $\text{CD}_3\text{CN}/\text{CDCl}_3$  (1:1) with associated solution structures. Red arrows highlight diagnostic variations in the chemical shifts for establishing the conformation of the azindol-pyridine unit, whereas blue arrows hold for the bipyridine unit (see text).

Within the frame of the site-binding approach,<sup>22</sup> the cumulative formation macroconstants (eqs 1 and 2) can be modeled with eqs 3 and 4, respectively.

$$\beta_{1,1}^{M,\text{L7}} = \sum_i \omega_{1,1(\text{N}_i)}^{\text{H,L7}} f_{\text{N}_i}^{M,\text{L7}} \quad (3)$$

$$\beta_{2,1}^{M,\text{L7}} = \sum_{i \neq j} \omega_{2,1(\text{N}_i\text{N}_j)}^{M,\text{L7}} (f_{\text{N}_i}^{M,\text{L7}}) (f_{\text{N}_j}^{M,\text{L7}}) u_{\text{L7}(\text{N}_i\text{N}_j)}^{M,M} \quad (4)$$

In these equations, the sums run over all microspecies possessing the same stoichiometry but differing by the precise location of the metallic cations bound to each specific nitrogen atom  $\text{N}_i$  (and  $\text{N}_j$ ) in ligand  $\text{L7}$ .  $\omega_{m,n}^{M,\text{L7}}$  takes into account the pure statistical (i.e., entropic) contribution due to change in molecular rotational entropies occurring upon complexation for each microspecies.<sup>23</sup> Once the point group of each partner contributing to eqs 1 and 2 is at hand,  $\omega_{m,n}^{M,\text{L7}}$  are easily computed using the method of symmetry numbers (see Figures S9 and S10 in the Supporting Information).  $f_{\text{N}_i}^{M,\text{L7}}$  corresponds to the absolute affinities of the  $\text{N}_i$  atom of the heterocyclic aromatic ring involved in the coordination of the cation. Application of the van't Hoff isotherm transforms these

thermodynamic descriptions into free energies of connection  $\Delta G_{\text{connect}, \text{N}_i}^{M,\text{L7}} = -RT \ln(f_{\text{N}_i}^{M,\text{L7}})$ , which include desolvation processes (the standard concentration of the reference state is set to 1 M).<sup>24</sup> Finally,  $u_{\text{L7}}^{M,M} = e^{-(\Delta E_{\text{L7}}^{M,M}/RT)}$  is the Boltzmann factor correcting for the free energy of connection for any intramolecular  $M \cdots M$  interactions resulting from the close location of the two cations in  $[\text{M}_2\text{L7}]^{2+}$ . Assuming that the affinity of distal and central N donors are identical ( $f_{\text{N-central}}^{M,\text{L7}} = f_{\text{N-distal}}^{M,\text{L7}} = f_{\text{connect}}^{M,\text{L7}}$ ), the application of eqs 3 and 4 provides eqs 5 and 6 for  $M = \text{H}^+$  (see Figures S9 and S10 in the Supporting Information) and eqs 7 and 8 for  $M = \text{Li}^+$  (see Figure S11 in the Supporting Information), from which pertinent microscopic thermodynamic descriptions can be computed (see Table 1, entries 3–6).<sup>25</sup>

$$\beta_{1,1}^{\text{H,L7}} = 2f_{\text{connect}}^{\text{H,L7}} \quad (5)$$

$$\beta_{2,1}^{\text{H,L7}} = 2(f_{\text{connect}}^{\text{H,L7}})^2 u_{\text{L7}}^{\text{H,H}} \quad (6)$$

$$\beta_{1,1}^{\text{Li,L7}} = 12f_{\text{connect}}^{\text{Li,L7}} \quad (7)$$

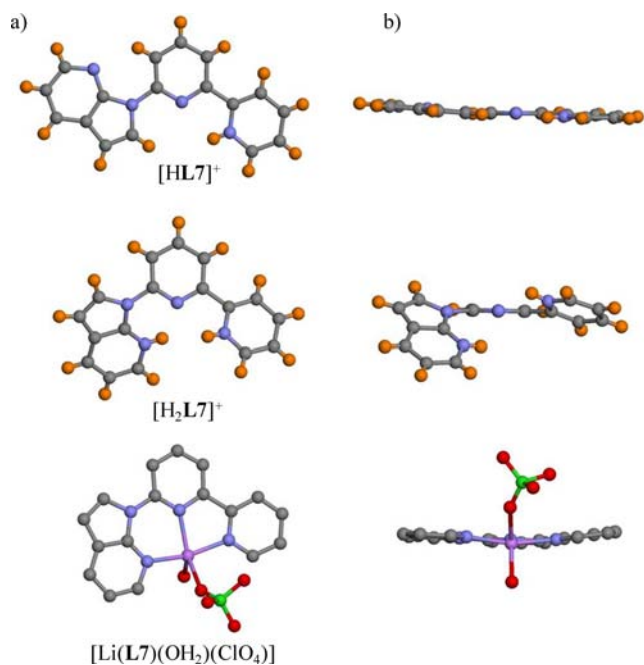


**Figure 3.** Perspective views (a) perpendicular and (b) parallel to the central pyridine ring of the molecular structures of  $[\text{HL7}]^+$ ,  $[\text{H}_2\text{L7}]^{2+}$  and  $[\text{Li}(\text{L7})(\text{OH}_2)(\text{ClO}_4)]$  observed in the crystal structures of  $[\text{HL7}](\text{CF}_3\text{SO}_3)$  (3),  $[\text{H}_2\text{L7}](\text{ClO}_4)_2$  (4) and  $[\text{Li}(\text{L7})(\text{ClO}_4)(\text{H}_2\text{O})]$  (5). Color code: gray = C, blue = N, orange = H, violet = Li. Hydrogen atoms are omitted for  $[\text{Li}(\text{L7})(\text{OH}_2)(\text{ClO}_4)]$ .

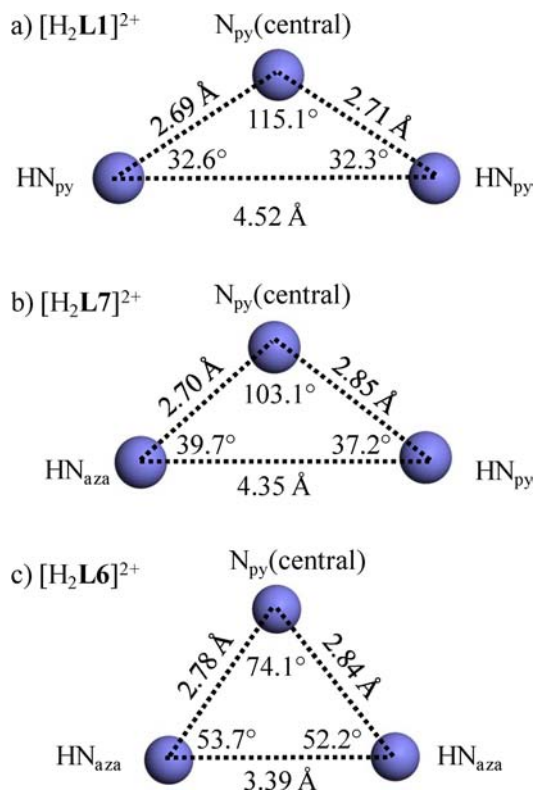
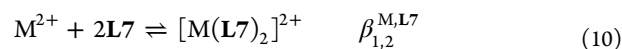
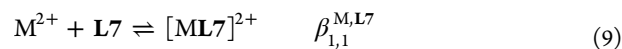


**Figure 4.** Geometries of the triangles formed by the donor N atoms in the molecular structures of (a)  $[\text{H}_2\text{L1}]^{2+}$ ,<sup>20</sup> (b)  $[\text{H}_2\text{L7}]^{2+}$ , and (c)  $[\text{H}_2\text{L6}]^{2+}$ .<sup>10</sup>

$$\beta_{2,1}^{\text{Li,L7}} = 144(f_{\text{connect}}^{\text{Li,L7}})^2 u_{\text{L7}}^{\text{Li,Li}} \quad (8)$$

The free energy of connection is much larger for the  $\text{H}^+$  cation than for the  $\text{Li}^+$  cation, because of the increase in size, which reduces the electrostatic factor to  $Z^2/R = 2.8 \text{ eu}/\text{\AA}$  for five-coordinated  $\text{Li}(\text{I})$ .<sup>26</sup> Interestingly, the unsymmetrical fused 5,6-membered chelate ligand **L7** displays the largest affinity for small univalent cation ( $\Delta G_{\text{connect}}^{\text{H,L7}} = -30.8(6) \text{ kJ/mol}$  and  $\Delta G_{\text{connect}}^{\text{Li,L7}} = -13.2(1.1) \text{ kJ/mol}$ ) compared with **L1** (fused 5,5-membered chelates,  $\Delta G_{\text{connect}}^{\text{H,L1}} = -16.7(6) \text{ kJ/mol}$  and  $\Delta G_{\text{connect}}^{\text{Li,L1}} > -5 \text{ kJ/mol}$ ) and **L6** (fused 6,6-membered chelates,  $\Delta G_{\text{connect}}^{\text{H,L6}} = -27.5(1.7) \text{ kJ/mol}$  and  $\Delta G_{\text{connect}}^{\text{Li,L6}} > -5 \text{ kJ/mol}$ ).<sup>10</sup> The successive protonations of **L1**, **L6**, and **L7** follow anticooperative protocols with a reluctance of  $6 < \Delta E_{\text{interaction}}^{\text{M,M,Lk}} < 9 \text{ kJ/mol}$  for the fixation of the second proton, while multilithiation in  $[\text{Li}_2\text{L7}]^{2+}$  is statistically within experimental uncertainties.

**Complexation of L7 with Divalent  $\text{Mg}^{2+}$  and  $\text{Zn}^{2+}$  Cations.** Electron spin ionization–mass spectroscopy (ESI-MS) titrations of **L7** with  $\text{M}^{2+}$  cation in acetonitrile show the initial formation of  $[\text{M}(\text{L7})]^{2+}$  ( $[\text{Mg}(\text{L7})(\text{CH}_3\text{CN})]^{2+}$  at  $m/z = 168.0$  and  $[\text{Zn}(\text{L7})]^{2+}$  at  $m/z = 169.4$ ), followed by the fixation of a second ligand to the divalent metal to give saturated  $[\text{M}(\text{L7})_2]^{2+}$  complexes ( $[\text{Mg}(\text{L7})_2]^{2+}$  at  $m/z = 284.0$  and  $[\text{Zn}(\text{L7})_2]^{2+}$  at  $m/z = 304.6$ ).  $^1\text{H}$  NMR titrations recorded in  $\text{CDCl}_3:\text{CD}_3\text{CN}$  or in  $\text{CD}_3\text{CN}$  operate under intermediate ( $\text{M} = \text{Mg}$ ; see Figure S12 in the Supporting Information) or slow ( $\text{M} = \text{Zn}$ , Figure S13 in the Supporting Information) exchange rate on the NMR time scale, which easily demonstrate that **L7**,  $[\text{ML7}]^{2+}$ , and  $[\text{M}(\text{L7})_2]^{2+}$  are the only ligand-containing species. Integration of the  $^1\text{H}$  NMR signals of the same proton in the different species provides quantitative speciations, from which the macroscopic stability constants for eqs 9 and 10 are deduced (see Table 1, columns 7–10, as well as Appendix I in the Supporting Information), together with ligand distributions (see Figure 5 and Figure S14 in the Supporting Information) and individual  $^1\text{H}$  NMR spectra (see Figure 6, as well as Figures S15 and S16 and Tables S1 and S2 in the Supporting Information). For  $\text{M} = \text{Mg}^{2+}$ , the considerable broadening of the signal at 298 K forced us to solve the speciations at 253 and 263 K (see Figures S17–S19 and Table S14 in the Supporting Information), from which the formation constants at 298 K collected in Table 1 were estimated by using linear van't Hoff plots with  $\ln(\beta_{1,1}^{\text{Mg,L7}}) = -(\Delta H_{1,1}^{\text{Mg,L7}})/RT + (\Delta S_{1,1}^{\text{Mg,L7}})/R$  ( $\Delta H_{1,1}^{\text{Mg,L7}}$  and  $\Delta S_{1,1}^{\text{Mg,L7}}$  are gathered in Table S14 in the Supporting Information).



The complexation of **L7** with either  $\text{Mg}^{2+}$  or  $\text{Zn}^{2+}$  is similar and shows the stepwise meridional tercoordination of two terdentate ligands to give the dynamically average  $C_s$ -symmetrical  $[\text{M}(\text{L7})]^{2+}$  and  $C_2$ -symmetrical  $[\text{M}(\text{L7})_2]^{2+}$  complexes on the NMR time scale. The systematic upfield shifts of H2, H3 and H9 are diagnostic for the transformation of the original *trans*–*trans* into *cis*–*cis* conformation for **L7** upon complexation, while the global downfield shifts of the protons bound at the para position of the pyridine rings (H1, H5 and H10) point to the complexation of the three N-donors to  $\text{M}^{2+}$  (see Figure 6 and Figures S15 and S16 in the Supporting Information).<sup>17</sup> It is worth noting here the unusual, but expected, upfield shifts by more than 1.0 ppm for H7 and H12 in  $[\text{M}(\text{L7})_2]^{2+}$ , which results from the location of these protons in the shielding

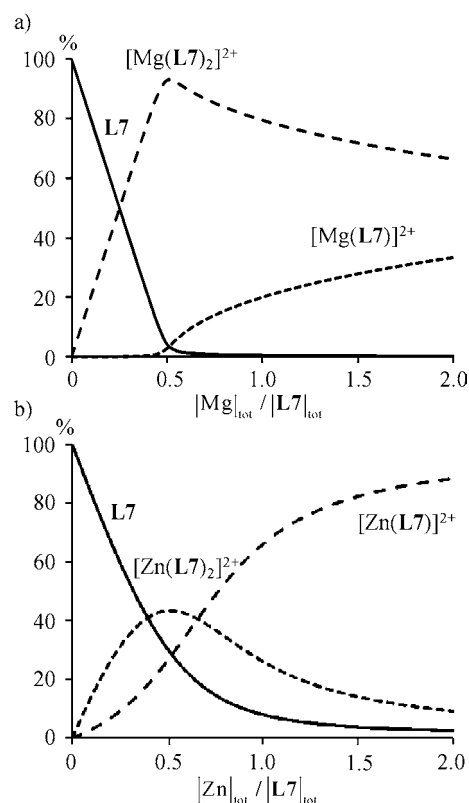


**Figure 5.** Computed ligand speciation (mole fraction (%)) of the ligand in the various species for the titrations of L7 with (a)  $\text{Mg}(\text{ClO}_4)_2$  and (b)  $\text{Zn}(\text{CF}_3\text{SO}_3)_2$  in  $\text{CD}_3\text{CN}/\text{CDCl}_3$  (1:1) at 298 K. Total ligand concentration  $|\text{L7}|_{\text{tot}} = 7.5 \times 10^{-3} \text{ M}$ .

domain of the pyridine ring of the adjacent ligand (see Figure 6, top).

X-ray crystal structures were solved for  $[\text{Mg}(\text{L7})(\text{OH}_2)_3](\text{ClO}_4)_2$  (**6**),  $[\text{Zn}(\text{L7})(\text{THF})(\text{CF}_3\text{SO}_3)_2]$  (**7**) and  $[\text{Zn}(\text{L7})_2]$

( $\text{CF}_3\text{SO}_3$ )<sub>2</sub>·0.13H<sub>2</sub>O (**8**). Each terdentate ligand is meridionally coordinated to the central cation in agreement with the solution structures deduced by NMR (see Figure 7, as well as Figure S20 and Tables S15–S21 in the Supporting Information). The bivalent metals are six-coordinated in pseudo-octahedral environments as found for analogous  $[\text{Mg}(\text{L1})(\text{OH}_2)_3]\text{Cl}_2$ ,<sup>27</sup>  $[\text{Zn}(\text{L1})(\text{S})\text{X}_2]$ <sup>28</sup> and  $[\text{Zn}(\text{L1})_2]\text{X}_2$  complexes.<sup>29</sup> However, the adjacent five- and six-membered chelates in L7 (instead of fused 5,5-membered chelates in L1) induces 15–20° helical twists along the polyaromatic strand in **6** and **7** as similarly observed for  $[\text{Li}(\text{L7})(\text{ClO}_4)(\text{H}_2\text{O})]$  (**5**), a distortion raised to 35°–45° in  $[\text{Zn}(\text{L7})_2]^{2+}$ , whereas the coordinated L1 ligands in  $[\text{Zn}(\text{L1})_2]^{2+}$  are essentially planar (Figure 7 and Figure S21 in the Supporting Information).<sup>29</sup> The average Mg–N and Zn–N bond distances are comparable for complexes with L1 and L7, but their specific distributions are different. With fused 5,5-membered chelates in L1, M(II) is located closer to the central pyridine ring (for instance  $\text{Mg}-\text{N}_{\text{pycentral}} = 2.12 \text{ \AA}$ ,  $\text{Mg}-\text{N}_{\text{pydistal}} = 2.20 \text{ \AA}$  in  $[\text{Mg}(\text{L1})(\text{OH}_2)_3]^{2+}$ ), whereas fused 5,6-membered chelate rings in L7 put M(II) at a remote distance from the central pyridine nitrogen donor atom, while the distal M–N interactions are shortened ( $\text{Mg}-\text{N}_{\text{pycentral}} = 2.20 \text{ \AA}$ ,  $\text{Mg}-\text{N}_{\text{pydistal}} = 2.13 \text{ \AA} \approx \text{Mg}-\text{N}_{\text{azadistal}} = 2.12 \text{ \AA}$  in  $[\text{Mg}(\text{L7})(\text{OH}_2)_3]^{2+}$ ).<sup>13a</sup> This effect is further amplified when two fused 6,6-membered chelate rings are coordinated to Zn(II) as reported for  $[\text{Zn}(\text{L6})(\text{CF}_3\text{SO}_3)_2]$  ( $\text{Zn}-\text{N}_{\text{pycentral}} = 2.25 \text{ \AA}$ ,  $\text{Zn}-\text{N}_{\text{azadistal}} = 2.00 \text{ \AA}$ ).<sup>10</sup>

The thermodynamic analysis of eqs 9 and 10 within the frame of the site-binding model<sup>22</sup> gives eqs 11 and 12 (see Figure S22 in the Supporting Information), from which the microscopic descriptors  $\Delta G_{\text{connect}}^{\text{M,L7}}$  and  $\Delta E_{\text{interaction}}^{\text{L7,L7M}}$  are computed (see Table 1, entries 3–6).

$$\beta_{1,1}^{\text{M,L7}} = 24f_{\text{connect}}^{\text{M,L7}} \quad (11)$$

$$\beta_{1,2}^{\text{M,L7}} = 24(f_{\text{connect}}^{\text{M,L7}})^2 u_{\text{M}}^{\text{L7,L7}} \quad (12)$$

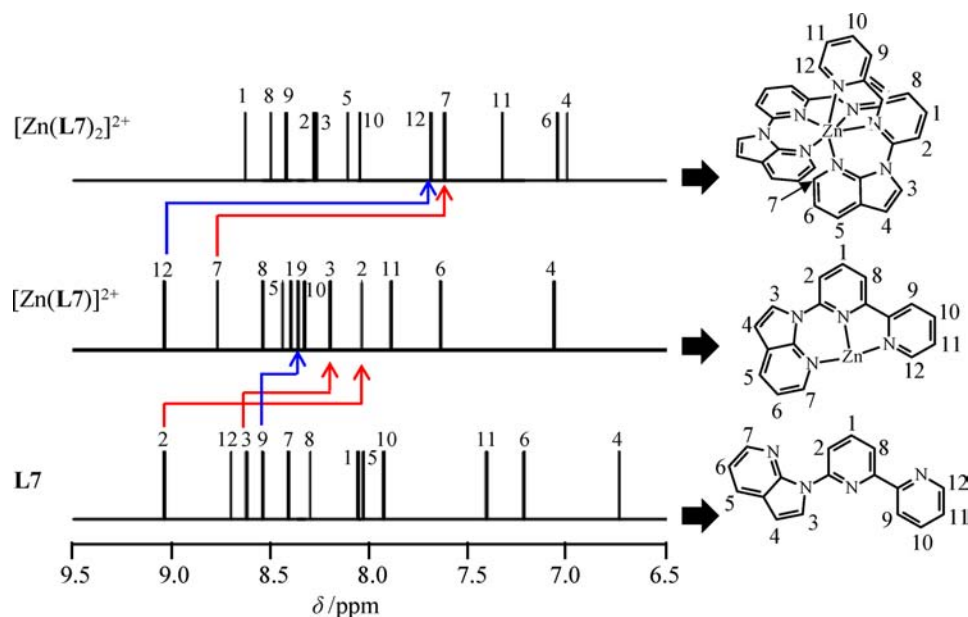


**Figure 6.** Computed individual <sup>1</sup>H NMR spectra for L7,  $[\text{Zn}(\text{L7})]^+$ , and  $[\text{Zn}(\text{L7})_2]^{2+}$  in  $\text{CD}_3\text{CN}/\text{CDCl}_3$  (1:1) with associated solution structures. Red arrows highlight chemical shifts variations diagnostic for establishing the conformation of the azaindol-pyridine unit, whereas blue arrows hold for the bipyridine unit (see text).

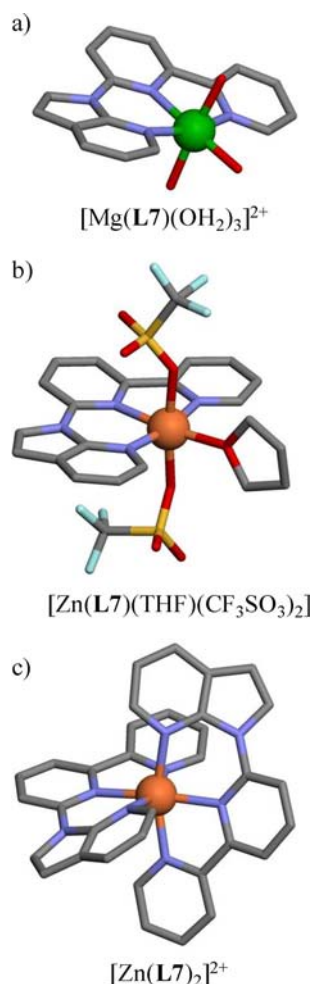
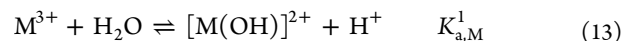


**Figure 7.** Perspective views of the molecular structures of (a) [Mg(L7)(OH<sub>2</sub>)<sub>3</sub>]<sup>2+</sup>, (b) [Zn(L7)(THF)(CF<sub>3</sub>SO<sub>3</sub>)<sub>2</sub>], and (c) [Zn(L7)<sub>2</sub>]<sup>2+</sup> observed in the crystal structures of [Mg(L7)(OH<sub>2</sub>)<sub>3</sub>](ClO<sub>4</sub>)<sub>2</sub> (6), [Zn(L7)(THF)(CF<sub>3</sub>SO<sub>3</sub>)<sub>2</sub>] (7), and [Zn(L7)<sub>2</sub>](CF<sub>3</sub>SO<sub>3</sub>)<sub>2</sub>·0.13H<sub>2</sub>O (8). Color code: gray = C, blue = N, red = O, yellow = S, light blue = F, green = Mg, pink = Zn. Hydrogen atoms are omitted for clarity.

Since the ionic radius of six-coordinate Mg<sup>2+</sup> (0.72 Å) and Zn<sup>2+</sup> (0.74 Å) are comparable,<sup>26</sup> their affinity for L7 is similar with  $\Delta G_{\text{connect}}^{\text{ML7}} \approx -15$  kJ/mol in CDCl<sub>3</sub>:CD<sub>3</sub>CN (1:1), a value reduced by 20%–30% in more-polar CD<sub>3</sub>CN. Surprisingly, the free energy of connection increases only slightly when going from M = Li<sup>+</sup> to Mg<sup>2+</sup>, despite the doubling of both positive charge and electrostatic factor. This suggests that solvation processes play a major role in the complexation reactions occurring in polar organic solvents, a statement substantiated by the enthalpy-penalized ( $\Delta H_{1,n}^{\text{ML7}} > 0$ ), but entropy-driven complexation processes ( $\Delta S_{1,n}^{\text{Mg,L7}} \gg 0$ ) revealed by van't Hoff plots for Mg<sup>2+</sup> (see Table S14 in the Supporting Information). We also notice that the fixation of the second terdentate ligand in [M(L7)<sub>2</sub>]<sup>2+</sup> is much more favorable for Mg<sup>2+</sup> (positive cooperativity  $\Delta E_{\text{interaction}}^{\text{L7,L7M}} \approx -15$  kJ/mol), while a rough statistical behavior is found for Zn<sup>2+</sup>, but the large uncertainties affecting this parameter for M = Mg prevent more-detailed interpretations.

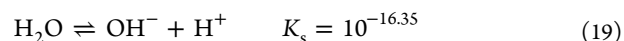
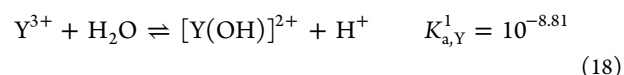
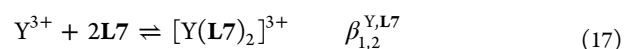
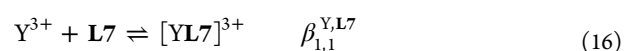
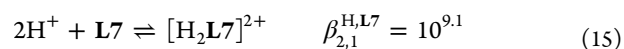
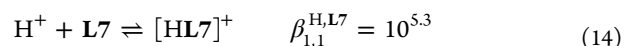
**Complexation of L7 with Trivalent Sc<sup>3+</sup>, La<sup>3+</sup>, and Y<sup>3+</sup> Cations.** Titration of L7 with hygroscopic Sc(CF<sub>3</sub>SO<sub>3</sub>)<sub>3</sub> in CD<sub>3</sub>CN shows the exclusive formation of the protonated ligand

[HL7]<sup>+</sup> and [H<sub>2</sub>L7]<sup>2+</sup> produced by the severe hydrolysis of small Sc<sup>3+</sup> with a trace of water, according to eq 13 (six-coordinate ionic radius  $R_{\text{Sc}}^{\text{CN}=6} = 0.75$  Å and  $\text{p}K_{\text{a,Sc}}^1 = 10^{-4.55}$  in water; see Figure S23 in the Supporting Information).<sup>26,30</sup>



In order to minimize water content, Sc(CF<sub>3</sub>SO<sub>3</sub>)<sub>3</sub> was replaced with anhydrous ternary complexes [La-(hfac)<sub>3</sub>(diglyme)]<sup>31</sup> and [Y(CF<sub>3</sub>SO<sub>3</sub>)<sub>3</sub>(diglyme)]<sup>32</sup> containing larger La<sup>3+</sup> (nine-coordinate ionic radius  $R_{\text{La}}^{\text{CN}=9} = 1.36$  Å,  $\text{p}K_{\text{a,La}}^1 = 10^{-9.01}$  in water, hfac = hexafluoroacetylacetonate) and Y<sup>3+</sup> cations ( $R_{\text{Y}}^{\text{CN}=9} = 1.08$  Å,  $\text{p}K_{\text{a,Y}}^1 = 10^{-8.81}$  in water).<sup>26,30</sup> Titration of L7 with [La(hfac)<sub>3</sub>(diglyme)] at millimolar concentrations in CD<sub>3</sub>CN displays only weak interactions and [La]<sub>tot</sub>/[L7]<sub>tot</sub> ratios larger than 5.0 are required for recording reliable changes in the <sup>1</sup>H NMR spectra (see Figure S24 in the Supporting Information).

The situation is different with [Y(CF<sub>3</sub>SO<sub>3</sub>)<sub>3</sub>(diglyme)], for which significant quantities of [Y(L7)]<sup>3+</sup> and [Y(L7)<sub>2</sub>]<sup>3+</sup> (slow exchange on the NMR time scale) are formed together with comparable amounts of protonated ligands [HL7]<sup>+</sup> and [H<sub>2</sub>L7]<sup>2+</sup> (fast exchange on the NMR time scale; see Figure S25 in the Supporting Information). The complete titration process can be satisfyingly modeled in CD<sub>3</sub>CN by simultaneously considering eqs 1, 2, 9, 10, and 13, adapted for M = Y<sup>3+</sup> (eqs 14–18), together with eq 19 for taking into account partial water dissociation in pure acetonitrile.<sup>33</sup> The fitting process used multi-Lorentzian deconvolutions of the complete <sup>1</sup>H NMR spectra, and it converged to  $\log(\beta_{1,1}^{\text{Y,L7}}) = 2.9(5)$  and  $\log(\beta_{1,2}^{\text{Y,L7}}) = 5.3(4)$  with the ligand distribution depicted in Figure 8 (see Appendix 2 in the Supporting Information).



According to the complicated speciation observed in solution, the isolation of pure yttrium complexes is difficult, but brownish X-ray quality crystals of [Y(L7)<sub>2</sub>Cl<sub>2</sub>]<sub>3</sub>·CH<sub>2</sub>Cl<sub>2</sub> (9) slowly deposited during the air evaporation of a CH<sub>3</sub>CN/CH<sub>2</sub>Cl<sub>2</sub> (1:8) solution containing YI<sub>3</sub>(THF)<sub>3,5</sub> (1 equiv)<sup>34</sup> and L7 (2 equiv; see Figure 9, as well as Figures S26 and S27, in addition to Tables S22–S24 in the Supporting Information).<sup>35</sup>

The 8-coordinated Y(III) metal in the [Y(L7)<sub>2</sub>Cl<sub>2</sub>]<sup>+</sup> cation is sandwiched between the two twisted terdentate ligands, with the two Cl<sup>−</sup> anions completing a pseudo-square antiprism (Figure 9). The Y–N bond distances (2.462–2.613 Å, average 2.54(7) Å) are similar to those reported for [Y(L1)(OH<sub>2</sub>)<sub>4</sub>Cl]<sup>2+</sup> (8-coordinate: 2.52(3) Å),<sup>36</sup> [Y(L1)(OH<sub>2</sub>)<sub>2</sub>(NO<sub>3</sub>)<sub>2</sub>]<sup>+</sup> (9-coordinate: 2.49(2) Å)<sup>37</sup> and [Y(L1)<sub>3</sub>]<sup>3+</sup> (9-coordinate: 2.52(3) Å).<sup>38</sup> However, the yttrium atom, which is located within the plane defined by the three coordinated donor N atoms for complexes with L1, lies at 1.187 and 1.197 Å from the related coordination planes in [Y(L7)<sub>2</sub>Cl<sub>2</sub>]<sup>+</sup> (Figure

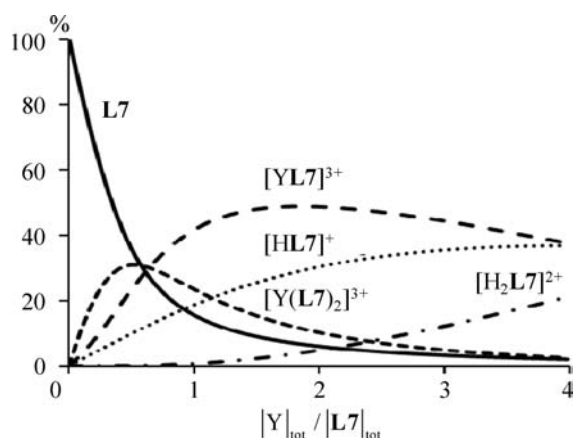


**Figure 8.** Computed ligand speciation for the titrations of L7 with  $[Y(\text{CF}_3\text{SO}_3)_3(\text{diglyme})]$  in  $\text{CD}_3\text{CN}$  at 298 K. Total ligand concentration  $[\text{L7}]_{\text{tot}} = 7.5 \times 10^{-3}$  M.

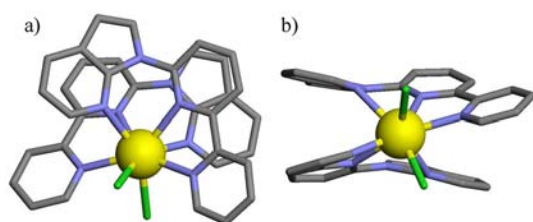


**Figure 9.** Perspective views (a) perpendicular and (b) parallel to the central pyridine ring of the terdentate ligands in the molecular structure of  $[Y(\text{L7})_2\text{Cl}_2]^+$  observed in the crystal structure of  $[Y(\text{L7})_2\text{Cl}_2]_3 \cdot \text{CH}_2\text{Cl}_2$  (9). Color code: gray = C, blue = N, green = Cl, yellow = Y. Hydrogen atoms are omitted for clarity.

9). This specific geometry is not the simple result of using 6-membered polyaromatic chelate rings, since a strictly planar  $\text{YN}_3$  core was recently reported for the complexation of a terdentate carbazole-bis(oxazoline) ligand possessing two fused 6,6-membered chelate rings.<sup>39</sup> We however note the operation of various intramolecular and intermolecular  $\pi$ -stacking interactions in  $[Y(\text{L7})_2\text{Cl}_2]^+$ , which could contribute to the stabilization of the observed sandwich conformation (see Figure S27 in the Supporting Information). The thermodynamic analysis of eqs 16 and 17 within the frame of the site-binding model<sup>22</sup> gives eqs 20 and 21 (Figure S28 in the Supporting Information), from which we can calculate a microscopic free energy of connection of  $\Delta G_{\text{connect}}^{\text{Y,L7}} = -12.1(2.9)$  kJ/mol for a noncooperative complexation process in  $\text{CD}_3\text{CN}$ ; this is a behavior very similar to that previously described for  $\text{Zn}^{2+}$  (Table 1, entries 3–6), but much less efficient than  $\Delta G_{\text{connect}}^{\text{Y,L1}} \approx \Delta G_{\text{connect}}^{\text{Y,L5}} = -30(3)$  kJ/mol reported for terdentate-fused 5,5-membered chelates in acetonitrile.<sup>2f</sup>

$$\beta_{1,1}^{\text{Y,L7}} = 6f_{\text{connect}}^{\text{Y,L7}} \quad (20)$$

$$\beta_{1,2}^{\text{Y,L7}} = 6(f_{\text{connect}}^{\text{Y,L7}})^2 u_{\text{Y}}^{\text{L7,L7}} \quad (21)$$

## CONCLUSION

The coordination chemistry of the semirigid polyaromatic terdentate ligands L1 (fused 5,5-chelates)<sup>5r</sup> and L6 (fused 6,6-chelates)<sup>10</sup> follows the geometrical rules established during the 1990s claiming that 5-membered chelate rings prefer large cations, whereas the reverse situation holds for 6-membered

chelates (see Figure S1 in the Supporting Information).<sup>1</sup> The intermediate structural characteristics provided by L7 (i.e., two fused 5,6-membered chelates) remove this effect in polar organic solvents. The terdentate ligand L7 indeed efficiently reacts with  $\text{H}^+$  ( $\Delta G_{\text{connect}}^{\text{H,L7}} \approx -30$  kJ/mol), and it displays significant affinities for  $\text{M} = \text{Li}^+, \text{Mg}^{2+}, \text{Zn}^{2+}$ , and  $\text{Y}^{3+}$  ( $\Delta G_{\text{connect}}^{\text{M,L7}} \approx -15$  kJ/mol to  $-10$  kJ/mol) without exhibiting pertinent dependence on the cationic electrostatic factors  $Z^2/R$ . Under these conditions, the use of easily hydrolyzed cations such as  $\text{Sc}^{3+}$  or  $\text{Y}^{3+}$ , in the presence of a trace of water, leads to unavoidable competition with protonation. Structurally speaking, this rough invariance of the affinity for various cations is correlated with their close interactions with the two distal donor N atoms, while the central N atom is remote. The opposite situation occurs for coordinated L1, which better encapsulates the incoming cations, thus optimizing enthalpic contributions. Therefore, it is not so surprising that the fixation of  $\text{Mg}^{2+}$  to L7 proved to be strictly entropy-driven with deleterious positive enthalpic contributions. This limitation could be overcome by using less-coordinating anhydrous organic solvents, as suggested by the systematic increase in binding affinity observed upon going from  $\text{CH}_3\text{CN}$  to  $\text{CH}_3\text{CN}:\text{CDCl}_3$  (1:1), and cyclic ethers are currently investigated for pushing this strategy forward. We finally note that the successive fixation of two monovalent cations to L7 is anticooperative, but the alternative binding of two ligands L7 to a single bivalent or tervalent cation may be driven by remarkable positive cooperativities.

## EXPERIMENTAL SECTION

Chemicals were purchased from Strem, Acros, Fluka AG, and Aldrich, and used without further purification, unless otherwise stated.  $\text{La}(\text{hfac})_3 \cdot \text{diglyme}$ ,<sup>31</sup>  $\text{Y}(\text{CF}_3\text{SO}_3)_3 \cdot \text{diglyme}$ <sup>32</sup> and  $\text{YI}_3(\text{THF})_{3.5}$ <sup>10,34</sup> were prepared according to literature procedures. Silicagel plates Merck 60 F<sub>254</sub> were used for thin layer chromatography (TLC) and Fluka silica gel 60 (0.04–0.063 mm) or Acros neutral activated alumina (0.050–0.200 mm) was used for preparative column chromatography.

**Preparation of 2-(tributylstannyl) Pyridine (1).** *n*-BuLi (8 mL, 1.6 M in hexane, 12.5 mmol) was added dropwise to a solution of 2-bromo pyridine (1.99 g, 12.5 mmol) in dry THF (5 mL) at  $-78$  °C, and the mixture was stirred for 1 h. Tributyltin chloride (3.4 mL, 12.65 mmol) was quickly added to the solution at  $-78$  °C, and stirring continued for 3 h at  $-78$  °C, then 30 min at room temperature. The reaction was quenched with saturated aqueous  $\text{NH}_4\text{Cl}$  solution (10 mL) and extracted with ethylacetate ( $3 \times 25$  mL). The combined organic layers were washed with brine, then water and finally dried over anhydrous  $\text{Na}_2\text{SO}_4$ . The solvent was evaporated under reduced pressure to give 2.7 g of 2-(tributylstannyl) pyridine (1, 12.5 mmol, yield = 99%) as a dark brown liquid.

<sup>1</sup>H NMR ( $\text{CDCl}_3$ , 400 MHz):  $\delta$  (ppm) 8.74–8.72 (m, 1H); 7.49 (dt, 1H); 7.40 (m, 1H); 7.09–7.13 (m, 1H); 1.57 (t, 6H); 1.30–1.35 (m, 6H); 1.10–1.14 (m, 6H); 0.88 (t, 9H). ESI-MS  $m/z$ : 370.18  $[\text{M} + \text{H}]^+$ .

**Preparation of 6-bromo-2,2'-bipyridine (2).** 2-(tributylstannyl) pyridine (1) (3.8 g, 10.32 mmol) was added to a degassed solution of 2,6-dibromo pyridine (2.6 g, 10.97 mmol) and  $\text{Pd}(\text{PPh}_3)_4$  (608 mg, 0.53 mmol) in toluene (4 mL). The mixture was refluxed under an inert atmosphere for 12 h, the solvent evaporated and the resulting residue dissolved in  $\text{CH}_2\text{Cl}_2$  (10 mL). Extraction with 6 M aq HCl ( $3 \times 10$  mL) provided an aqueous layer, which was carefully neutralized with 10% aq ammonia (60 mL) at 0 °C, then extracted with dichloromethane ( $3 \times 30$  mL). The combined organic layers were washed with water and dried over anhydrous  $\text{Na}_2\text{SO}_4$ . The solvent was evaporated and the resulting solid residue was purified by column chromatography ( $\text{CH}_2\text{Cl}_2/\text{MeOH}$ : 99.5/0.5  $\rightarrow$  99/1) yielded 1.3 g of



6-bromo-2,2'-bipyridine (**2**, 5.5 mmol, yield = 53%) as a white solid.  $^1\text{H}$  NMR ( $\text{CDCl}_3$ , 400 MHz):  $\delta$  (ppm) 8.69 (m, 1H); 8.43 (td, 1H,  $^3J = 8.0$  Hz); 8.40 (dd, 1H,  $^3J = 7.6$  Hz,  $^4J = 0.8$  Hz); 7.84 (dt, 1H,  $^3J = 7.6$  Hz,  $^4J = 2$  Hz); 7.69 (t, 1H,  $^3J = 8.0$  Hz); 7.51 (dd, 1H,  $^3J = 8.0$  Hz,  $^4J = 0.8$  Hz); 7.35 (m, 1H). ESI-MS,  $m/z$ : 235.1 [ $\text{M}+\text{H}$ ] $^+$ .

**Preparation of 6-(azaindol-1-yl)-2,2'-bipyridine (L7).** 6-Bromo-2,2'-bipyridine (866 mg, 3.6 mmol), 7-azaindole (390 mg, 3.30 mmol),  $\text{K}_2\text{CO}_3$  (993 mg, 7.2 mmol), trans-1,2-diaminocyclohexane (41 mg, 0.36 mmol), and CuI (35 mg, 0.18 mmol) in dioxane (10 mL) were degassed with  $\text{N}_2$  for 30 min. The mixture was then refluxed under an inert atmosphere for 72 h. The solvent was evaporated, and the resulting brown residue was extracted with  $\text{CH}_2\text{Cl}_2$  ( $3 \times 40$  mL) and washed with water. The organic layer was dried over  $\text{MgSO}_4$ , and the solvent was evaporated under reduced pressure. The resulting solid was purified by column chromatography ( $\text{CH}_2\text{Cl}_2/\text{MeOH}$ : 99/1) to yield 787 mg of 6-(azaindol-1-yl)-2,2'-bipyridine (**L7**, 2.9 mmol, yield = 87%) as a white solid.  $^1\text{H}$  NMR ( $\text{CDCl}_3$ , 400 MHz):  $\delta$  9.02 (dd, 1H,  $^3J = 8.2$  Hz,  $^4J = 0.8$  Hz); 8.73 (m, 1H); 8.60 (d, 1H,  $^3J = 3.6$  Hz); 8.53 (td, 1H,  $^3J = 7.6$  Hz,  $^4J = 1.2$  Hz); 8.45 (dd, 1H,  $^3J = 4.8$  Hz,  $^4J = 1.6$  Hz); 8.32 (dd, 1H,  $^3J = 7.6$  Hz,  $^4J = 0.8$  Hz); 8.03 (t, 1H,  $^3J = 8.0$  Hz); 8.0 (dd, 1H,  $^3J = 8.0$  Hz,  $^4J = 1.6$  Hz); 7.88 (dt, 1H,  $^3J = 7.6$  Hz,  $^4J = 2$  Hz); 7.36 (d, 1H,  $^3J = 4.8$  Hz); 7.20 (dd, 1H,  $^3J = 8.0$  Hz,  $^4J = 4.8$  Hz); 6.70 (d, 1H,  $^3J = 4$  Hz).  $^{13}\text{C}$  NMR ( $\text{CDCl}_3$ , 100 MHz):  $\delta$  156.82 (Cquat); 154.58 (Cquat); 150.16 (Cquat); 149.21 (C12); 147.69 (Cquat); 143.16 (C7); 139.35 (C1); 136.88 (C10); 129.07 (C5); 126.44 (C3); 123.84 (C11); 123.39 (Cquat); 121.23 (C9); 117.42 (C8); 117.20 (C6); 115.63 (C2); 102.56 (C4). ESI-MS ( $\text{CH}_2\text{Cl}_2$ ):  $m/z$  272.93 [ $\text{M}+\text{H}$ ] $^+$ . Elemental analyses: Calcd for  $\text{C}_{17}\text{H}_{12}\text{N}_4$ : C 74.98%, H 4.44%, N 20.58%. Found C 74.63%, H 4.31%, N 20.30%.

**Preparation of the Complexes. [HL7](CF<sub>3</sub>SO<sub>3</sub>) (3).** Diethyl ether was slowly diffused into a concentrated solution containing **L7** (1 equiv) and  $\text{HCF}_3\text{SO}_3$  (1 equiv) in  $\text{CH}_3\text{CN}/\text{CH}_2\text{Cl}_2$  (1:1) to give X-ray quality prisms of [HL7](CF<sub>3</sub>SO<sub>3</sub>).

[H<sub>2</sub>L7](ClO<sub>4</sub>)<sub>2</sub> (4). The dissolution of **L7** (10 mg, 0.037 mmol) in acetonitrile/dichloromethane (1:1, 1 mL), followed by the addition of 6 M aq HClO<sub>4</sub> (16  $\mu\text{L}$ , 0.093 mmol) resulted in the precipitation of [H<sub>2</sub>L7](ClO<sub>4</sub>)<sub>2</sub>. The solid was filtered, washed with dichloromethane, diethyl ether and dried under vacuum to afford a 13 mg of [H<sub>2</sub>L7](ClO<sub>4</sub>)<sub>2</sub> (0.027 mmol, yield 74%) as a white solid. Slow diffusion of THF into a concentrated solution containing **L7** (1 equiv) and HClO<sub>4</sub> (2 equiv) in  $\text{CH}_3\text{CN}/\text{CH}_2\text{Cl}_2$  (1:1) gave X-ray quality prisms of [H<sub>2</sub>L7](ClO<sub>4</sub>)<sub>2</sub> (4).  $^1\text{H}$  NMR ( $\text{CD}_3\text{CN}$ , 400 MHz):  $\delta$  8.94 (d,  $^3J = 3.6$  Hz, 1H); 8.88 (dd,  $^3J = 8.0$  Hz,  $^4J = 1.0$  Hz, 1H); 8.82 (dt,  $^3J = 7.8$  Hz, 1H); 8.71 (d,  $^3J = 7.8$  Hz, 1H); 8.60 (d,  $^3J = 6.0$  Hz, 1H); 8.48 (t,  $^3J = 8.1$  Hz, 1H); 8.35 (d,  $^3J = 7.8$  Hz, 1H); 8.28 (d,  $^3J = 3.8$  Hz, 1H); 8.22 (t,  $^3J = 7.2$  Hz, 1H); 8.07 (d,  $^3J = 8.3$  Hz, 1H, H2); 7.83 (dd,  $^3J = 7.9$  Hz,  $^4J = 6.0$  Hz, 1H, H6); 7.26 (d,  $^3J = 3.8$  Hz, 1H, H4). Elemental analysis: Calcd:  $\text{C}_{17}\text{H}_{14}\text{N}_4\text{Cl}_2\text{O}_8$  ([H<sub>2</sub>L7](ClO<sub>4</sub>)<sub>2</sub>): C, 43.15; H, 2.98; N, 11.83. Found: C, 43.00; H, 3.00; N, 11.90.

[Li(L7)(OH<sub>2</sub>)(ClO<sub>4</sub>)] (5). Heptane was slowly diffused into a concentrated solution containing **L7** (1 equiv) and LiClO<sub>4</sub> (1 equiv) in  $\text{CH}_3\text{CN}/\text{CH}_2\text{Cl}_2$  (1:1) to give X-ray quality prisms of [Li(L7)(OH<sub>2</sub>)(ClO<sub>4</sub>)].

[MgL7](ClO<sub>4</sub>)<sub>2</sub>·3H<sub>2</sub>O (6). Stoichiometric amounts of **L7** (10 mg, 0.037 mmol) and Mg(ClO<sub>4</sub>)<sub>2</sub> (8.3 mg, 0.037 mmol) were dissolved in acetonitrile/dichloromethane (1:1, 1 mL). The solvent was partially evaporated and slow diffusion of diethyl ether afforded 5 mg of X-ray quality prisms of [MgL7](ClO<sub>4</sub>)<sub>2</sub>·3H<sub>2</sub>O (0.009 mmol, yield 25%).  $^1\text{H}$  NMR ( $\text{CD}_3\text{CN}$ , 400 MHz):  $\delta$  8.87 (d,  $^3J = 4.5$  Hz, 1H); 8.63 (dd,  $^3J = 5.3$  Hz,  $^4J = 1.4$  Hz, 1H); 8.54 (d,  $^3J = 8.2$  Hz, 1H), 8.45 (dd,  $^3J = 7.8$  Hz,  $^4J = 1.5$  Hz, 1H); 8.42 (t,  $^3J = 8.1$  Hz, 1H); 8.40 (dt,  $^3J = 8.0$  Hz,  $^4J = 1.5$  Hz, 1H); 8.34 (dt,  $^3J = 7.7$  Hz,  $^4J = 1.6$  Hz, 1H); 8.22 (d,  $^3J = 4.1$  Hz, 1H); 8.05 (dd,  $^3J = 7.7$  Hz,  $^4J = 1.5$  Hz, 1H); 7.85 (ddd,  $^3J = 7.6$  Hz,  $^4J = 5.2$  Hz,  $^5J = 0.9$  Hz, 1H); 7.62 (dd,  $^3J = 7.9$ ,  $^4J = 5.3$  Hz, 1H); 7.09 (d,  $^3J = 4.1$  Hz, 1H). Elemental analysis: Calcd for  $\text{MgC}_{17}\text{H}_{18}\text{N}_4\text{Cl}_2\text{O}_{11}$ : C, 37.15; H, 3.30; N, 10.19. Found: C, 37.28; H, 3.32; N, 10.04.

[Zn(L7)](CF<sub>3</sub>SO<sub>3</sub>)<sub>2</sub> (7). Stoichiometric amounts of **L7** (10 mg, 0.037 mmol) and Zn(CF<sub>3</sub>SO<sub>3</sub>)<sub>2</sub> (13.45 mg, 0.037 mmol) were dissolved in

acetonitrile (0.5 mL). The slow diffusion of tetrahydrofuran (THF), followed by filtration and drying, afforded 12 mg [ZnL7](CF<sub>3</sub>SO<sub>3</sub>)<sub>2</sub> (0.019 mmol, yield 51%) as a white microcrystalline powder. Slow diffusion of THF into a concentrated solution containing **L7** (1 equiv) and Zn(CF<sub>3</sub>SO<sub>3</sub>)<sub>2</sub> (1 equiv) in  $\text{CH}_3\text{CN}$  gave X-ray quality prisms of [Zn(L7)](CF<sub>3</sub>SO<sub>3</sub>)<sub>2</sub> (7).  $^1\text{H}$  NMR ( $\text{CD}_3\text{CN}$ , 400 MHz):  $\delta$  9.04 (d,  $^3J = 6$  Hz, 1H); 8.78 (dd,  $^3J = 5.4$  Hz,  $^4J = 1.4$  Hz, 1H); 8.60 (td,  $^3J = 7.3$  Hz, 1H); 8.50 (dd,  $^3J = 7.8$  Hz,  $^4J = 1.5$  Hz, 1H); 8.44 (t,  $^3J = 7.7$  Hz, 1H); 8.42 (dt,  $^3J = 7.7$  Hz,  $^4J = 2$  Hz, 1H); 8.40 (dt,  $^3J = 7.6$  Hz,  $^4J = 1.6$  Hz, 1H); 8.27 (d,  $^3J = 4.1$  Hz, 1H); 8.09 (dd,  $^3J = 7.7$  Hz,  $^4J = 1.6$  Hz, 1H); 7.93 (ddd,  $^3J = 7.7$  Hz,  $^4J = 5.3$  Hz,  $^5J = 1.0$  Hz, 1H); 7.68 (dd,  $^3J = 7.8$ ,  $^4J = 5.4$  Hz, 1H); 7.12 (d,  $^3J = 4.08$  Hz, 1H). Elemental analysis: Calcd for  $\text{ZnC}_{19}\text{H}_{17}\text{N}_4\text{F}_6\text{O}_6$ : C, 35.89; H, 1.90; N, 8.81. Found: C, 35.50; H, 2.19; N, 8.71.

[Zn(L7)<sub>2</sub>](CF<sub>3</sub>SO<sub>3</sub>)<sub>2</sub> (8). Stoichiometric amounts of **L7** (10 mg, 0.037 mmol) and Zn(CF<sub>3</sub>SO<sub>3</sub>)<sub>2</sub> (6.7 mg, 0.019 mmol) were dissolved in acetonitrile/dichloromethane (1:1, 1 mL). The solvent was then partially evaporated. Slow diffusion of THF afforded 4 mg of X-ray quality prisms of [Zn(L7)<sub>2</sub>](CF<sub>3</sub>SO<sub>3</sub>)<sub>2</sub> (0.004 mmol, yield 24%).  $^1\text{H}$  NMR ( $\text{CD}_3\text{CN}$ , 400 MHz)  $\delta$  8.64 (7,  $^3J = 8.1$  Hz, 1H); 8.51 (d,  $^3J = 7.8$  Hz, 1H); 8.43 (d,  $^3J = 8.2$  Hz, 1H); 8.30–8.27 (m, 2H, H2); 8.13 (dd,  $^3J = 7.8$  Hz,  $^4J = 1.4$  Hz, 1H); 8.05 (dt,  $^3J = 8.0$  Hz,  $^4J = 1.6$  Hz, 1H); 7.76 (d,  $^3J = 5.0$  Hz, 1H); 7.71 (d,  $^3J = 6.6$  Hz, 1H); 7.33 (dd,  $^3J = 6.8$  Hz,  $^4J = 5.8$  Hz, 1H); 7.04 (dd,  $^3J = 7.8$  Hz,  $^4J = 5.3$  Hz, 1H); 7.02 (d,  $^3J = 4.1$  Hz, 1H). Elemental analysis: Calcd for  $\text{ZnC}_{36}\text{H}_{24}\text{N}_8\text{S}_2\text{F}_6\text{O}_6$ : C, 47.61; H, 2.66; N, 12.33. Found: C, 46.75; H, 3.00; N, 11.60.

[Y(L7)<sub>2</sub>Cl<sub>2</sub>]<sub>3</sub>·CH<sub>2</sub>Cl<sub>2</sub> (9). Brownish X-ray quality crystals of [Y(L7)<sub>2</sub>Cl<sub>2</sub>]<sub>3</sub>·CH<sub>2</sub>Cl<sub>2</sub> (9) slowly deposited during the air evaporation of a concentrated  $\text{CH}_3\text{CN}/\text{CH}_2\text{Cl}_2$  (1:8) solution containing YI<sub>3</sub>(THF)<sub>3.5</sub> (1 equiv) and **L7** (2 equiv).

**Spectroscopic Measurements.**  $^1\text{H}$  and  $^{13}\text{C}$  NMR spectra were recorded on a Bruker Avance 400 MHz spectrometer. Chemical shifts are given in parts per million (ppm), with respect to TMS. In a typical  $^1\text{H}$  NMR titration experiment, 500  $\mu\text{L}$  of a  $7.5 \times 10^{-3}$  M solution of ligand **L7** in  $\text{CD}_3\text{CN}/\text{CDCl}_3$  (1:1) were reacted with successive aliquots of solutions of CF<sub>3</sub>SO<sub>3</sub>H, LiClO<sub>4</sub>, Mg(ClO<sub>4</sub>)<sub>2</sub>, Zn(CF<sub>3</sub>SO<sub>3</sub>)<sub>2</sub>, or Y(CF<sub>3</sub>SO<sub>3</sub>)<sub>2</sub>-diglyme in the same solvent mixture. After each aliquot, the  $^1\text{H}$  NMR spectrum was recorded at 298 K and the global chemical shifts matrix was fitted to pertinent equilibria using the HypNMR-2008 software.<sup>16</sup> Pneumatically assisted electrospray ionization–mass spectroscopy (ESI-MS) spectra were recorded from  $10^{-4}$  M solutions on an Applied Biosystems API 150EX LC/MS System equipped with a Turbo Ionspray source. Elemental analyses were performed by K. L. Buchwalder from the Microchemical Laboratory of the University of Geneva.

**X-ray Crystallography.** Summary of crystal data, intensity measurements, and structure refinements for [HL7](CF<sub>3</sub>SO<sub>3</sub>) (3), [H<sub>2</sub>L7](ClO<sub>4</sub>)<sub>2</sub> (4), [Li(L7)(OH<sub>2</sub>)(ClO<sub>4</sub>)] (5), Mg(L7)(OH<sub>2</sub>)<sub>3</sub>·(ClO<sub>4</sub>)<sub>2</sub> (6), [Zn(L7)(THF)(CF<sub>3</sub>SO<sub>3</sub>)<sub>2</sub>] (7), [Zn(L7)<sub>2</sub>](CF<sub>3</sub>SO<sub>3</sub>)<sub>2</sub>·0.13H<sub>2</sub>O (8), and [Y(L7)<sub>2</sub>Cl<sub>2</sub>]<sub>3</sub>·CH<sub>2</sub>Cl<sub>2</sub> (9) were collected in Tables S4, S15, and S22 in the Supporting Information. All crystals were mounted on quartz fibers with protection oil. Cell dimensions and intensities were measured at 180 or 293 K on an Agilent Supernova diffractometer with mirror-monochromated Cu- $[\text{K}\alpha]$  radiation ( $\lambda = 1.54184$  Å). Data were corrected for Lorentz and polarization effects and for absorption. The structures were solved by direct methods (SIR97),<sup>40</sup> all other calculation were performed with ShellX97<sup>41</sup> systems and ORTEP3<sup>42</sup> programs. CCDC-926740 to CCDC-926747 (3–9) contain the supplementary crystallographic data. The CIF files can be obtained free of charge via www.ccdc.cam.ac.uk/conts/retrieving.html (or from the Cambridge Crystallographic Data Centre, 12 Union Road, Cambridge CB2 1EZ, U.K.; fax: (+44) 1223-336-033; or deposit@ccdc.cam.ac.uk).

## ■ ASSOCIATED CONTENT

### Supporting Information

Methods of speciation (Appendixes 1 and 2). Tables of  $^1\text{H}$  NMR chemical shifts, crystal data, geometric parameters, bond

distances and bond angles, and thermodynamic data. Figures showing molecular structures with numbering schemes and crystal packing,  $^1\text{H}$  NMR titrations, ligand speciations and applications of the site binding model. A CIF file for compounds  $[\text{HL7}](\text{CF}_3\text{SO}_3)$  (3),  $[\text{H}_2\text{L7}](\text{ClO}_4)_2$  (4),  $[\text{Li}(\text{L7})(\text{OH}_2)(\text{ClO}_4)]$  (5),  $\text{Mg}(\text{L7})(\text{OH}_2)_3(\text{ClO}_4)_2$  (6),  $[\text{Zn}(\text{L7})(\text{THF})(\text{CF}_3\text{SO}_3)_2]$  (7),  $[\text{Zn}(\text{L7})_2](\text{CF}_3\text{SO}_3)_2 \cdot 0.13\text{H}_2\text{O}$  (8), and  $[\text{Y}(\text{L7})_2\text{Cl}_2]_3 \cdot \text{CH}_2\text{Cl}_2$  (9). This material is available free of charge via the Internet at <http://pubs.acs.org>.

## AUTHOR INFORMATION

### Corresponding Author

\*E-mail addresses: [Claude.Piguet@unige.ch](mailto:Claude.Piguet@unige.ch) (C.P.), [Thi.Hoang@unige.ch](mailto:Thi.Hoang@unige.ch) (T.H.Y.H.).

### Notes

The authors declare no competing financial interest.

## ACKNOWLEDGMENTS

Financial support from the Swiss National Science Foundation is gratefully acknowledged.

## REFERENCES

- (1) (a) Hancock, R. D. *J. Chem. Educ.* **1992**, *69*, 615–621. (b) Motekaitis, R. J.; Martell, A. E.; Hancock, R. D. *Coord. Chem. Rev.* **1994**, *133*, 39–65 and references therein.
- (2) For reviews, see: (a) Bünzli, J.-C. G. In *Handbook on the Physics and Chemistry of Rare Earths*, Vol. 10; Gschneider, K. A., Jr., Eyring, L., Eds.: Elsevier: Amsterdam, 1987; pp 322–394. (b) Sabbatini, N.; Guardigli, M.; Lehn, J.-M. *Coord. Chem. Rev.* **1993**, *123*, 201–228. (c) Gawryszewska, P.; Sokolnicki, J.; Legendziewicz, J. *Coord. Chem. Rev.* **2005**, *249*, 2489–2509. (d) Bünzli, J.-C. G. *Acc. Chem. Res.* **2006**, *39*, 53–61. (e) Comby, S.; Bünzli, J.-C. G. In *Handbook on the Physics and Chemistry of Rare Earths*, Vol. 37; Gschneider, K. A., Jr., Bünzli, J.-C. G., Pecharsky, V. K., Eds.; Elsevier Science: Amsterdam, 2007; pp 217–470. (f) Piguet, C.; Bünzli, J.-C. G. In *Handbook on the Physics and Chemistry of Rare Earths*, Vol. 40; Gschneider, K. A., Jr., Bünzli, J.-C. G., Pecharsky, V. K., Eds.; Elsevier Science: Amsterdam, 2009; pp 301–553. (g) Moore, E. G.; Samuel, A. P. S.; Raymond, K. N. *Acc. Chem. Res.* **2009**, *42*, 542–552. (h) Eliseeva, S. V.; Bünzli, J.-C. G. *Chem. Soc. Rev.* **2010**, *39*, 189–227. (i) Eliseeva, S. V.; Bünzli, J.-C. G. *New J. Chem.* **2011**, *35*, 1165–1176. (j) Xu, J.; Corneille, T. M.; Moore, E. G.; Law, G.-L.; Butlin, N. G.; Raymond, K. N. *J. Am. Chem. Soc.* **2011**, *133*, 19900–19910.
- (3) For reviews, see: (a) Benelli, C.; Gatteschi, D. *Chem. Rev.* **2002**, *102*, 2369–2387. (b) Sorace, L.; Benelli, C.; Gatteschi, D. *Chem. Soc. Rev.* **2011**, *40*, 3092–3104. (c) Luzon, J.; Sessoli, R. *Dalton Trans.* **2012**, *41*, 13556–13567.
- (4) (a) Senegas, J.-M.; Bernardinelli, G.; Imbert, D.; Bünzli, J.-C. G.; Morgantini, P.-Y.; Weber, J.; Piguet, C. *Inorg. Chem.* **2003**, *42*, 4680–4695. (b) Zou, J.; Berg, D. J.; Stuart, D.; McDonald, R.; Twamley, B. *Organometallics* **2011**, *30*, 4958–4967.
- (5) (a) Durham, D. A.; Frost, G. H.; Hart, F. A. *J. Inorg. Nucl. Chem.* **1969**, *31*, 833–838. (b) Chapman, R. D.; Loda, R. T.; Riehl, J. P.; Schwartz, R. W. *Inorg. Chem.* **1984**, *23*, 1652–1657. (c) Fréchette, M.; Bensimon, C. *Inorg. Chem.* **1995**, *34*, 3520–3527. (d) Semenova, L. I.; White, A. H. *Aust. J. Chem.* **1999**, *52*, 507–517. (e) Semenova, L. I.; Sobolev, A. N.; Skelton, B. W.; White, A. H. *Aust. J. Chem.* **1999**, *52*, 519–529. (f) Bekiari, V.; Lianos, P. *Adv. Mater.* **2000**, *12*, 1603–1605. (g) Drew, M. G. B.; Iveson, P. B.; Hudson, M. J.; Liljenzin, J. O.; Spjuth, L.; Cordier, P.-Y.; Enarsson, A.; Hill, C.; Madic, C. *J. Chem. Soc., Dalton Trans.* **2000**, 821–830. (h) Mürner, H.-R.; Chassat, E.; Thummel, R. P.; Bünzli, J.-C. G. *J. Chem. Soc., Dalton Trans.* **2000**, 2809–2816. (i) Rabbe, C.; Mikhalko, V.; Dognon, J.-P. *Theor. Chem. Acc.* **2000**, *104*, 280–283. (k) Ahrens, B.; Cotton, S. A.; Feeder, N.; Noy, O. E.; Raithby, P. R.; Teat, S. J. *J. Chem. Soc., Dalton Trans.* **2002**, 2027–2030. (l) Berthet, J.-C.; Rivière, C.; Miquel, Y.; Nierlich, M.; Madic, C.; Ephritikhine, M. *Eur. J. Inorg. Chem.* **2002**, 1439–1446. (m) Fukuda, Y.; Nakao, A.; Hayashi, K. *J. Chem. Soc., Dalton Trans.* **2002**, 527–533. (n) Cotton, S. A.; Franckevicius, V.; How, R. E.; Ahrens, B.; Ooi, L. L.; Mahon, M. F.; Raithby, P. R.; Teat, S. J. *Polyhedron* **2003**, *22*, 1489–1497. (o) Guillaumont, D. *J. Phys. Chem. A* **2004**, *108*, 6893–6900. (p) Berthet, J.-C.; Nierlich, M.; Miquel, Y.; Madic, C.; Ephritikhine, M. *Dalton Trans.* **2005**, 369–379. (q) Sénéchal-David, K.; Hemeryck, A.; Tancrez, N.; Toupet, L.; Williams, J. A. G.; Ledoux, I.; Zyss, J.; Boucekine, A.; Guégan, J.-P.; Le Bozec, H.; Maury, O. *J. Am. Chem. Soc.* **2006**, *128*, 12243–12255. (r) Petit, L.; Daul, C.; Adamo, C.; Maldivi, P. *New J. Chem.* **2007**, *31*, 1738–1745. (s) Hamilton, J. M.; Anhorn, M. J.; Oscarson, K. A.; Reibenspies, J. H.; Hancock, R. D. *Inorg. Chem.* **2011**, *50*, 2764–2770. (t) de Bettencourt-Dias, A.; Bauer, S.; Viswanathan, S.; Maull, B. C.; Ako, A. M. *Dalton Trans.* **2012**, *41*, 11212–11218. (u) Di Bernardo, P.; Melchior, A.; Tolazzi, M.; Zanonato, P. L. *Coord. Chem. Rev.* **2012**, *256*, 328–351.
- (6) (a) Drew, M. G. B.; Hudson, M. J.; Iveson, P. B.; Madic, C.; Russel, M. L. *J. Chem. Soc., Dalton Trans.* **2000**, 2711–2720. (b) Boubals, N.; Drew, M. G. B.; Hill, C.; Hudson, M. J.; Iveson, P. B.; Madic, C.; Russell, M. L.; Youngs, T. G. A. *J. Chem. Soc., Dalton Trans.* **2002**, 55–62. (c) Karmazin, L.; Mazzanti, M.; Gateau, C.; Hill, C.; Pécaut, J. *Chem. Commun.* **2002**, 2892–2893. (d) Drew, M. G. B.; Hill, C.; Hudson, M. J.; Iveson, P. B.; Madic, C.; Youngs, T. G. A. *Dalton Trans.* **2004**, 244–251. (e) Foreman, M. R. S.; Hudson, M. J.; Drew, M. G. B.; Hill, C.; Madic, C. *Dalton Trans.* **2006**, 1645–1653. (f) Hudson, M. J.; Boucher, C. E.; Braekers, D.; Desreux, J. F.; Drew, M. G. B.; Foreman, M. R. S. J.; Harwood, L. M.; Hill, C.; Madic, C.; Marken, F.; Youngs, T. G. A. *New J. Chem.* **2006**, *30*, 1171–1183. (g) Hubscher-Bruder, V.; Haddaoui, J.; Bouhroum, S.; Arnaud-Neu, F. *Inorg. Chem.* **2010**, *49*, 1363–1371.
- (7) (a) Bardwell, D. A.; Jeffery, J. C.; Jones, P. L.; McCleverty, J. A.; Psillakis, E.; Reeves, Z.; Ward, M. D. *J. Chem. Soc., Dalton Trans.* **1997**, 2079–2086. (b) Kadjane, P.; Starck, M.; Camerel, F.; Hill, D.; Hildebrandt, N.; Ziessel, R.; Charbonnière, L. *J. Inorg. Chem.* **2009**, *48*, 4601–4603. (c) Bremer, A.; Ruff, C. M.; Girnt, D.; Müllich, U.; Rothe, J.; Roesky, P. W.; Panak, P. J.; Karpov, A.; Müller, T. J. J.; Denecke, M. A.; Geist, A. *Inorg. Chem.* **2012**, *51*, 5199–5207.
- (8) (a) de Bettencourt-Dias, A.; Barber, P. S.; Viswanathan, S.; de Lill, D. T.; Rollett, A.; Ling, G.; Altun, S. *Inorg. Chem.* **2010**, *49*, 8848–8861. (b) Matsumoto, K.; Suzuki, K.; Tsukuda, T.; Tsubomura, T. *Inorg. Chem.* **2010**, *49*, 4717–4719. (c) Yuasa, J.; Ohno, T.; Miyata, K.; Tsumatori, H.; Hasegawa, Y.; Kawai, T. *J. Am. Chem. Soc.* **2011**, *133*, 9892–9902. (d) Ward, M. D.; Gade, L. H. *Chem. Commun.* **2012**, *48*, 10587–10599.
- (9) (a) Piguet, C.; Williams, A. F.; Bernardinelli, G.; Moret, E.; Bünzli, J.-C. G. *Helv. Chim. Acta* **1992**, *75*, 1697–1717. (b) Piguet, C.; Bünzli, J.-C. G.; Bernardinelli, G.; Williams, A. F. *Inorg. Chem.* **1993**, *32*, 4139–4149. (c) Piguet, C.; Bünzli, J.-C. G.; Bernardinelli, G.; Bochet, C. G.; Froidevaux, P. *J. Chem. Soc., Dalton Trans.* **1995**, 83–97. (d) Petoud, S.; Bünzli, J.-C. G.; Renaud, F.; Piguet, C.; Schenk, K. J.; Hopfgartner, G. *Inorg. Chem.* **1997**, *36*, 5750–5760. (e) Petoud, S.; Bünzli, J.-C. G.; Schenk, K. J.; Piguet, C. *Inorg. Chem.* **1997**, *36*, 1345–1353. (f) Ionova, G.; Rabbe, C.; Guillaumont, R.; Ionov, S.; Madic, C.; Krupa, J.-C.; Guillauneux, D. *New J. Chem.* **2002**, *26*, 234–242. (g) Froidevaux, P.; Harrowfield, J. M.; Sobolev, A. N. *Inorg. Chem.* **2000**, *39*, 4678–4687. (h) Nozary, H.; Piguet, C.; Rivera, J.-P.; Tissot, P.; Bernardinelli, G.; Vulliermet, N.; Weber, J.; Bünzli, J.-C. G. *Inorg. Chem.* **2000**, *39*, 5286–5298. (i) Muller, G.; Bünzli, J.-C. G.; Schenk, K. J.; Piguet, C.; Hopfgartner, G. *Inorg. Chem.* **2001**, *40*, 2642–2651. (j) Muller, G.; Riehl, J. P.; Schenk, K. J.; Hopfgartner, G.; Piguet, C.; Bünzli, J.-C. G. *Eur. J. Inorg. Chem.* **2002**, 3101–3110. (k) Beck, J. B.; Rowan, S. J. *J. Am. Chem. Soc.* **2003**, *125*, 13922–13923. (l) Drew, M. G. B.; Hill, C.; Hudson, M. J.; Iveson, P. B.; Madic, C.; Vaillant, L.; Youngs, T. G. A. *New J. Chem.* **2004**, *28*, 462–470. (m) Terazzi, E.; Torelli, S.; Bernardinelli, G.; Rivera, J.-P.; Bénech, J.-M.; Bourgogne, C.; Donnio, B.; Guillon, D.; Imbert, D.; Bünzli, J.-C. G.; Pinto, A.; Jeannerat, D.; Piguet, C. *J. Am. Chem. Soc.* **2005**, *127*, 888–903. (n) Knapton, D.; Iyer, P. K.; Rowan, S. J.; Weder, C. *Macromolecules*

- 2006, 39, 4069–4075. (o) Burnworth, M.; Knapton, D.; Rowan, S. J.; Weder, C. J. *Inorg. Organomet. Polym. Mater.* **2007**, 17, 91–103. (p) Escande, A.; Guéneé, L.; Buchwalder, K.-L.; Pigué, C. *Inorg. Chem.* **2009**, 48, 1132–1147. (q) Shavaleev, N. M.; Scopelliti, R.; Gumy, F.; Bünzli, J.-C. G. *Inorg. Chem.* **2009**, 48, 2908–2918. (r) Shavaleev, N. M.; Scopelliti, R.; Gumy, F.; Bünzli, J.-C. G. *Inorg. Chem.* **2009**, 48, 6178–6191. (s) Shavaleev, N. M.; Scopelliti, R.; Gumy, F.; Bünzli, J.-C. G. *Inorg. Chem.* **2009**, 48, 7937–7946. (t) Shavaleev, N. M.; Gumy, F.; Scopelliti, R.; Bünzli, J.-C. G. *Inorg. Chem.* **2009**, 48, 5611–5613. (u) Shavaleev, N. M.; Eliseeva, S. V.; Scopelliti, R.; Bünzli, J.-C. G. *Inorg. Chem.* **2010**, 49, 3929–3936.
- (10) Hoang, T. N.; Lathion, T.; Guéneé, L.; Terazzi, E.; Pigué, C. *Inorg. Chem.* **2012**, 51, 8567–8575.
- (11) Collins, S. N.; Taylor, S.; Krause, J. A.; Connick, W. B. *Acta Crystallogr., Sect. C: Cryst. Struct. Commun.* **2007**, C63, m436–m439.
- (12) Zhao, Q.-L.; Li, G.-P. *Acta Crystallogr., Sect. E: Struct. Rep. Online* **2009**, E65, m693.
- (13) The related, but less-flexible, aromatic fused 5–6 membered terdentate ligand 2-(8′quinolinyl)-1,10-phenanthroline has been reported to react with Pt(II) and Ru(II) to give distorted tetragonal and pseudo-octahedral complexes. (a) Hu, Y.-Z.; Wilson, M. H.; Zong, R.; Bonnefous, C.; McMillin, D. R.; Thummel, R. P. *Dalton Trans.* **2005**, 354–358. (b) Kaveevivitchai, N.; Zong, R.; Tseng, H.-W.; Chitta, R.; Thummel, R. P. *Inorg. Chem.* **2012**, 2930–2939.
- (14) Shin, D.; Switzer, C. *Chem. Commun.* **2007**, 4401–4403.
- (15) (a) Sperotto, E.; van Klink, G. P. M.; van Koten, G.; de Vries, J. G. *Dalton Trans.* **2010**, 39, 10338–10351. (b) Garner, K. L.; Parkes, J. F.; Piper, J. D.; Williams, J. A. G. *Inorg. Chem.* **2010**, 49, 476–487.
- (16) HypNMR-2008 software: (a) Frassinetti, C.; Ghelli, S.; Gans, P.; Sabatini, A.; Moruzzi, M. S.; Vacca, A. *Anal. Biochem.* **1995**, 231, 374–382. (b) Frassinetti, C.; Alderighi, L.; Gans, P.; Sabatini, A.; Vacca, A.; Ghelli, S. *Bioanal. Chem.* **2003**, 376, 1041–1052.
- (17) Lavalée, D. K.; Baughman, M. D.; Phillips, M. D. *J. Am. Chem. Soc.* **1977**, 99, 718–724.
- (18) (a) Reimers, J. R.; Hall, L. E. *J. Am. Chem. Soc.* **1999**, 121, 3730–3744. (b) Constable, E. C.; Doyle, M. J.; Healy, J.; Raithby, P. R. *J. Chem. Soc., Chem. Commun.* **1988**, 1262–1263.
- (19) The nitrogen atom of the central pyridine and the two coordinated oxygen atoms form the trigonal basis.
- (20) (a) Kepert, C. J.; Skelton, B. W.; White, A. H. *Aust. J. Chem.* **1994**, 47, 391–396. (b) Drew, M. G. B.; Hudson, M. J.; Iveson, P. B.; Russell, M. L.; Lilijenzin, J.-O.; Skälberg, M.; Spjuth, L.; Madic, C. J. *Chem. Soc., Dalton Trans.* **1998**, 2973–2980. (c) Berthon, C.; Grigoriev, M. S. *Acta Crystallogr., Sect. E: Struct. Rep. Online* **2005**, E61, o1216–o1217.
- (21) Ercolani, G.; Schiaffino, L. *Angew. Chem., Int. Ed.* **2011**, 50, 1762–1768.
- (22) (a) Hamacek, J.; Borkovec, M.; Pigué, C. *Chem.—Eur. J.* **2005**, 11, 5227–5237. (b) Hamacek, J.; Borkovec, M.; Pigué, C. *Chem.—Eur. J.* **2005**, 11, 5217–5226. (c) Hamacek, J.; Borkovec, M.; Pigué, C. *Dalton Trans.* **2006**, 1473–1490. (d) Pigué, C. *Chem. Commun.* **2010**, 46, 6209–6231.
- (23) Ercolani, G.; Pigué, C.; Borkovec, M.; Hamacek, J. *J. Phys. Chem. B* **2007**, 111, 12195–12203.
- (24) (a) Schwarzenbach, G. *Helv. Chim. Acta* **1952**, 35, 39–65. (b) Adamson, A. W. *J. Am. Chem. Soc.* **1954**, 76, 1578–1579. (c) Martell, A. E. *Adv. Chem. Ser.* **1966**, 62, 272–294. (d) Munro, D. *Chem. Brit.* **1977**, 13, 100–105. (e) Simmons, E. L. *J. Chem. Educ.* **1979**, 56, 578–579. (f) Chung, C.-S. *J. Chem. Educ.* **1984**, 61, 1062–1064.
- (25) In eqs 5 and 6, we assume that  $f_{\text{connect}}^{\text{H,L7}} = f_{\text{N}_{\text{py,distal}}}^{\text{H,L7}} = f_{\text{N}_{\text{py,central}}}^{\text{H,L7}} = f_{\text{N}_{\text{az,distal}}}^{\text{H,L7}}$  and  $u_{\text{L7}}^{\text{H,H}} = u_{\text{L7}}^{\text{H}_{\text{N}_{\text{py,central}}}, \text{H}_{\text{N}_{\text{az,distal}}}} = u_{\text{L7}}^{\text{H}_{\text{N}_{\text{py,distal}}}, \text{H}_{\text{N}_{\text{az,distal}}}}$ .
- (26) (a) Shannon, R. D. *Acta Crystallogr., Sect. A: Cryst. Phys., Diffr., Theor. Gen. Crystallogr.* **1976**, A32, 751–767. (b) D’Angelo, P.; Zitolo, A.; Migliorati, V.; Chillemi, G.; Duvail, M.; Vitorge, P.; Abadie, S.; Spezia, R. *Inorg. Chem.* **2011**, 50, 4572–4579.
- (27) (a) Waters, A. F.; White, A. H. *Aust. J. Chem.* **1996**, 49, 147. (b) Bock, C. W. *Inorg. Chem.* **1994**, 33, 419–427.
- (28) (a) Einstein, F. W. B.; Penfold, B. R. *Acta Crystallogr.* **1966**, 20, 924–926. (b) Vlasse, M.; Rojo, T.; Beltran-Porter, D. *Acta Crystallogr., Sect. C: Cryst. Struct. Commun.* **1983**, C39, 560–563. (c) Harrison, P. G.; Begley, M. J.; Kikabhai, T.; Killer, F. J. *Chem. Soc., Dalton Trans.* **1986**, 929–934. (d) Tamasi, G.; Cini, R. *Dalton Trans.* **2003**, 2928–2936. (e) Finn, R. C.; Zubieta, J. J. *Chem. Soc., Dalton Trans.* **2002**, 856–861. (f) Shalumova, T.; Tanski, J. M. *Acta Crystallogr., Sect. E: Struct. Rep. Online* **2009**, E65, m1325. (g) Zhao, Q.-L.; Li, G.-P. *Acta Crystallogr., Sect. E: Struct. Rep. Online* **2009**, E65, m693.
- (29) (a) Harvey, M. A.; Baggio, S.; Ibanez, A.; Baggio, R. *Acta Crystallogr., Sect. C: Cryst. Struct. Commun.* **2004**, C60, m375–m381. (b) Dumitru, F.; Petit, E.; Van der Lee, A.; Barboiu, M. *Eur. J. Inorg. Chem.* **2005**, 4255–4262. (c) Tang, L.; Yang, X.-G.; Li, D.-S.; Wang, J.-J.; Gao, X.-M.; Wang, J.-W.; Kristallogr., Z. *New Cryst. Struct.* **2007**, 222, 59. (d) Goforth, A. M.; Tershansy, M. A.; Smith, M. D.; Peterson, L.; Kelley, J. G.; DeBenedetti, W. J. I. H.; Loye, C. Z. *J. Am. Chem. Soc.* **2011**, 133, 603–612.
- (30) Baes, C. F. J.; Mesmer, R., E. *Hydrolysis of Cations*; Wiley-Interscience: New York, 1976; Ch. 7, p 129.
- (31) (a) Evans, W. J.; Giarikos, D. G.; Johnston, M. A.; Greci, M. A.; Ziller, J. W. *J. Chem. Soc., Dalton Trans.* **2002**, 4, 520–526. (b) Malandrino, G.; Nigro, R. L.; Fragala, I. L.; Cristiano, B. *Eur. J. Inorg. Chem.* **2004**, 3, 500–509.
- (32) Aspinall, H. C.; Greeves, N.; McIver, E. G. *J. Alloys Compd.* **1998**, 275–277, 773–776.
- (33) Kilic, E.; Aslan, N. *Microchim. Acta* **2005**, 151, 89–92.
- (34) Izod, K.; Liddle, S. T.; Clegg, W. *Inorg. Chem.* **2004**, 43, 214–218.
- (35) The noncoordinated triiodide  $\text{I}_3^-$  counteranion is produced by air oxidation of iodide, whilst the chloride anion probably results from halide exchange reactions between  $\text{CH}_2\text{Cl}_2$  and  $\text{I}^-$ .
- (36) Kepert, C. J.; Weimin, L.; Skelton, B. W.; White, A. H. *Aust. J. Chem.* **1994**, 47, 365–384.
- (37) Semenova, L. I.; White, A. H. *Aust. J. Chem.* **1999**, 52, 507–517.
- (38) Semenova, L. I.; Sobolev, A. N.; Skelton, B. W.; White, A. H. *Aust. J. Chem.* **1999**, 52, 519–529.
- (39) Zou, J.; Berg, D. J.; Stuart, D.; McDonald, R.; Twamley, B. *Organometallics* **2011**, 30, 4958–4967.
- (40) Altomare, A.; Burla, M. C.; Camalli, M.; Casciarano, G.; Giacovazzo, C.; Guagliardi, A.; Moliterni, G.; Polidori, G.; Spagna, R. *J. Appl. Crystallogr.* **1999**, 32, 115–119.
- (41) Sheldrick, G. M. *SHELXL97 Program for the Solution and Refinement of Crystal Structures*; University of Göttingen, Göttingen, Germany, 1997.
- (42) ORTEP3 for Windows: Farrugia, L. J. *J. Appl. Crystallogr.* **1997**, 30, 565–566.